A Methyl-, Acetyl- and Allyl-palladium and -Platinum Complexes Containing Novel Terdentate PNS and NN'S Ligands

Ankersmit, H.A.; Veldman, N.; Spek, A.L.; Vrieze, K.; van Koten, G.

DOI
10.1016/S0020-1693(96)05333-9

Publication date
1996

Published in
Inorganica Chimica Acta

ELSEVIER

Inorganica Chimica Acta 252 (1996) 339–354

Inorganica Chimica Acta

Methyl-, acetyl- and allyl-palladium and -platinum complexes containing novel terdentate PNS and NN'S ligands

Hubertus A. Ankersmit [a], Nora Veldman [b], Anthony L. Spek [b,1], Kees Vrieze, [a,*], Gerard van Koten [c]

[a] *J.H. van 't Hoff Research Institute, Vakgroep Anorganische Chemie, Universiteit van Amsterdam, Nieuwe Achtergracht 166, 1018 WV Amsterdam, Netherlands*

[b] *Bijvoet Centre for Biomolecular Research, Vakgroep Kristal- en Structuurchemie, Universiteit Utrecht, Padualaan 8, 3584 CH Utrecht, Netherlands*

[c] *Debye Institute, Department of Metal-Mediated Synthesis, Universiteit Utrecht, Padualaan 8, 3584 CH Utrecht, Netherlands*

Received 5 May 1996; revised 10 June 1996

Abstract

Palladium and platinum compounds of the composition [MX(L)]X and [M(Me)(L)]X (M = Pd, Pt; X = Cl, Br, I, O_3SCF_3) have been prepared from the appropriate starting materials and the new ligands (L = *N*-[2-(diphenylphosphino)benzylidene]-*L*-methioninol (PNS-1), *N*-[2-(diphenylphosphino)benzylidene]-3-propylethylsulfide (PNS-2), *N*-{*N*-[2-(diphenylphosphino)benzylidene]-*D*/*L*-methio-nyl}-*tert*-butylamine (PNS-3), *N*-{*N*-[2-(pyridine)methylidene]-*D*/*L*-methionyl}-*tert*-butylamine (NN'S)). The single crystal X-ray determination of [PtI(PNS-3)]I (**3cz**) (triclinic, space group $P\bar{1}$ (No. 2) with $a = 10.5298(9)$, $b = 11.5584(8)$, $c = 14.545(2)$ Å, $\alpha = 77.368(8)$, $\beta = 84.453(9)$, $\gamma = 79.720(7)°$, $V = 1696.5(3)$ Å^3, $Z = 2$, $R1 = 0.0456$, $wR2 = 0.1195$) showed terdentate coordination of the trifunctional PNS-3 ligand with a six-membered PN containing metallacycle and a six-membered NS containing metallacycle which is in a chair conformation. The square planar geometry is completed with an iodide atom, while the second iodide atom is non-coordinating. The methyl-palladium and -platinum complexes may occur in solution in various isomeric forms, as an equilibrium has been observed between the ionic [M(Me)(η^3-PNS)]X and the neutral [MX(Me)(η^2-PNS)]. The η^3-PNS bonded complex may occur in two conformations, i.e. with the six-membered NS containing part of the ligand in either the chair or boat form. The methyl-palladium and -platinum complexes reacted slowly with CO to form the corresponding acetyl complexes, with insertion rates which increased in the order Cl < Br < I < $O_3SCF_3^-$ and PNS-1 < PNS-2 < PNS-3 < NN'S. Complexes [Pd(η^3-allyl)(PNS-3)]X (X = Cl, O_3SCF_3) with 2-methylallyl and 1,1,2-trimethylallyl groups have been prepared from the reaction of [PdCl(η^3-allyl)]$_2$ with PNS-3. Both the η^3-allyl and the unusual η^1-allyl species have been identified by ^{1}H NMR and their dynamic properties have been investigated in $CDCl_3$.

Keywords: Palladium complexes; Platinum complexes; Terdentate ligand complexes; Alkyl complexes; Allyl complexes; Acetyl complexes

1. Introduction

In our laboratory the *N*-[*N*-(5-methyl-2-thienylmethylidene)-*L*-methionyl]histamine ligand was designed in order to mimic the active site of plastocyanine [1]. In the solid state this hemilabile ligand shows a polymeric structure which is formed by inter- and intramolecular hydrogen bonds [2]. The $CH_2CH_2SCH_3$ arm connected to the central chiral methionic carbon atom is stretched out and a helix geometry is formed. Upon coordination to a cationic silver(I) or copper(I) nucleus again a polymeric helix geometry is created as each of the hemilabile ligand molecules binds to three metal ions while each metal center is bonded to three different hemilabile ligands. In solution this polymeric structure dissociates into oligomers of varying size, while the coordination mode of the ligand is unchanged. The geometry of the ligand backbone in the complex in the solid state as well as in solution is only slightly changed when compared to the structure of the free ligand, which means that the tetrahedral geometry of the coordination site is mainly ligand controlled, for non-discriminating ions like Ag(I) and Cu(I) [3].

This interesting feature initiated our interest in the coordination behavior of this ligand towards d^8-metal centers which favor a square planar instead of a tetrahedral geometry and which would be expected to force the ligand into a different conformation. In order to attain more understanding about the coordination properties of this ligand, the coordi-

* Corresponding author.

[1] To whom correspondence should be sent with regards to the crystallographic data.

PII S0020-1693(96)05333-9

nation behavior of the [*N*-(thienylidene)-*L*/*D*-methionyl] and of the methionine parts of the ligand were studied separately.

Coordination of the NSS′ [*N*-(thienylidene)-*L*/*D*-methionyl]methyl ester ligand towards Pd(II) showed a preference for bidentate coordination via the imine nitrogen and methionine sulfur donor atoms, while the thienyl sulfur donor is positioned above the coordination plane [4]. The geometry of the ligand backbone is changed appreciably owing to the position of the thienyl moiety and the preference of the Pd(II) atom for a square planar surrounding. It was shown that the rate of insertion of CO into the Pd–Me bond of the methylpalladium complexes [PdX(Me)(*D*/*L*-th-metMe-*N*,*S*)] was greatly enhanced by the η^2-bonded NS ligand, when compared to complexes containing bi- and terdentate nitrogen ligands [5]. In the course of these investigations we also discovered that the insertion of CO, in the Pd–Me bond of [PdCl(Me)(*D*/*L*-th-metMe-*N*,*S*)] in the presence of H_2O, caused the hydrolysis of the imine bond to an amine group, resulting in the formation of the novel and unexpectedly stable complex [PdCl(C(O)Me)(L)] (L = methionine methyl ester) [6] in which the ligand is bidentate bonded via the amine nitrogen as well as the methionine thioether sulfur atom, similar to [Pt(*L*-MetH-*S*,*N*)Cl_2], [$PtCl_2$(*L*/*D*-MetH-*S*,*N*)] [7] and [$PdCl_2$(*L*/*D*-MetH-*S*,*N*)] [8]. This unexpected finding prompted us to take a closer look at simple bidentate NS and NN′ ligands containing a hard amine function combined with either a soft S–Me or a soft pyridine moiety. It was found that both the bidentate NS and NN′ ligands enhance both CO and allene insertion rates even more than the afore-mentioned NSS′ ligand, while the insertion of (substituted) allenes into the Pd–Me bond affording η^3-allyl complexes could be studied in greater detail.

The observation that the thienyl moiety of the [*N*-(thienylidene)-*L*/*D*-methionyl]methyl ester ligand does not coordinate to the palladium center of [PdX(Me)(*D*/*L*-th-metMe-*N*,*S*)], not even when an open site on the metal center is created by halide abstraction, i.e. [Pd(Me)(*D*/*L*-th-metMe-*N*,*S*)](O_3SCF_3), prompted us to investigate ligand systems containing a donor atom such as a phosphorus and a pyridine nitrogen atom instead of the thienyl sulfur donor.

Here we report on the coordination behavior of the *N*-[2-(diphenylphosphino)benzylidene]-3-propylethylsulfide (PNS-1), *N*-[2-(diphenylphosphino)benzylidene]-*L*-methioninol (PNS-2), *N*-{*N*-[2-(diphenylphosphino)benzylidene]-*D*/*L*-methionyl}-tert-butylamine (PNS-3) and *N*-{*N*-[2-(pyridine)methylidene]-*D*/*L*-methionyl}-tert-butylamine (NN′S) ligands (Fig. 1) towards palladium(II) and platinum(II), resulting in ionic complexes of the type [MX(L)]Y (L = PNS, NN′S; M = Pd, Pt; X = Cl, Br, I, Me; Y = Cl, Br, I, OTf). The dynamic behavior of the ligand backbone in the complexes is studied by variable temperature ^{1}H and ^{31}P{^{1}H} NMR.

The reactivity of the methyl containing complexes towards CO is investigated as a function of: (i) the anion (Cl, Br or I); (ii) the donor atom linked to the NS backbone (N or P); (iii) the alkyl group bonded to the sulfur donor (Me or Et); (iv) the bulkiness of the group on the C-4 carbon atom of the NS backbone (H, CH_2OH, C(O)NH-tBu).

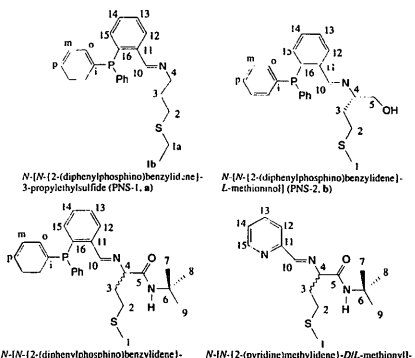

Fig. 1. A schematic presentation of the PNS and NN′S ligands.

2. Experimental

2.1. Materials

All reactions were carried out in an atmosphere of purified nitrogen, using standard Schlenk techniques. Solvents were carefully dried and distilled prior to use or stored under an inert atmosphere, unless denoted otherwise. [$PdCl_2$(COD)], [Pd(Me)Cl(COD)] (COD = cyclo-1,5-octadiene) [9], 2-diphenylphosphine-benzaldehyde [10], [PdCl(η^3-CH_2C(Me)CH_2)]$_2$ and [PdCl(η^3-CH_2C(Me)C(Me)$_2$)]$_2$ [5], γ-aminopropyl-ethylsulfide (H_2N-Prop-S-Et) [11] [2] and *N*-tert-butyloxycarbonyl-*L*-methionine (BOC-Met-OH) [12] were synthesized by literature procedures. Methioninol, 2-tert-butyloxycarbonyloximino-2-phenylacetonitrile (BOC-ON), methionine and 2-pyridine carboxaldehyde are commercially available and were used without further purification.

2.2. Instrumentation

^{1}H, ^{31}P{^{1}H}, ^{13}C{^{1}H} and ^{15}N{^{1}H}-INEPT spectra were recorded on Bruker AMX 300 and AC 100 spectrometers. Chemical shift values are in ppm relative to Me_4Si (^{1}H and ^{13}C{^{1}H}), 85% H_3PO_4 (^{31}P{^{1}H}) and CH_3NO_2 (^{15}N{^{1}H}-

[2] ^{1}H NMR ($CDCl_3$, 293 K, δ): 1.22 (t, 3H, S–CH_2CH_3); 1.70 (q, 2H, H_2N–$CH_2CH_2CH_2$); 2.4–2.6 (m, 4H, CH_2–S–CH_2); 2.77 (t, 2H, H_2N–CH_2). ^{13}C{^{1}H} NMR ($CDCl_3$, 293 K, δ): 15.2 (S–CH_2CH_3); 26.4 (S–CH_2CH_3); 29.3 (H_2N–$CH_2CH_2CH_2$); 33.8 (H_2N–$CH_2CH_2CH_2$); 41.7 (H_2N–$CH_2CH_2CH_2$) was not reported in Refs. [11a] and [11b].

INEPT). Coupling constants are in Herz (Hz). IR spectra were recorded on a Biorad spectrophotometer in the range 1000–2200 cm^{-1}.

The degree of association of **4cy** was calculated from vapor pressure measurements with a Hewlett-Packard osmometer 320B in dichloromethane (instrumental error amounts to 5%). Conductivity experiments were carried out using a Consort K720 digital conductometer.

The CO insertion rates were determined employing a sapphire tube (10.0 mm outer diameter, 8.0 mm inner diameter) [13]. Prior to the NMR experiment, the tube was shaken twice, while connected to the CO pressure line, in order to dissolve CO homogeneously. The CO insertion reaction was monitored by $^{31}P\{^1H\}$ and ^1H NMR at room temperature, employing approximately 0.02 M solutions ($CDCl_3$) of the methylpalladium complexes, and 10 bar CO.

Elemental analyses were carried out by Dornis und Kolbe, Muhlheim a.d. Ruhr in Germany.

2.3. Crystal structure determination of 3cz

Crystal data and details on data collection and refinement of compound **3cz** are presented in Table 1. A yellowish crystal was picked out of solution, cut to size and mounted on a Lindemann-glass capillary and transferred into the cold nitrogen stream on an Enraf-Nonius CAD4-T diffractometer on rotating anode. Accurate unit-cell parameters and an orientation matrix were determined by least-squares refinement of 25 reflections (SET4 [14]) in the range $11.7 < \theta < 13.7°$. The unit-cell parameters were checked for the presence of higher lattice symmetry [15]. Data were corrected for Lp effects. Three periodically measured reference reflections showed no significant decay during 21 h of X-ray exposure time. An empirical absorption and extinction correction was applied (DIFABS [16], correction range 0.76–1.28). The structure was solved by automated Patterson methods and subsequent difference Fourier techniques (DIRDIF-92 [17]). Refinement on F^2 was carried out by full-matrix least-squares techniques (SHELXL-93 [18]); no observance criterion was applied during refinement. All non-hydrogen atoms were refined with anisotropic thermal parameters. Hydrogen atoms were taken into account at calculated positions and refined riding on their carrier atoms, with fixed isotropic thermal parameter amounting to 1.5 to 1.2 times the value of the equivalent isotropic thermal parameter of their carrier atoms, for methyl hydrogen atoms, and all other hydrogen atoms, respectively. Weights were optimized in the final refinement cycles. Convergence was reached at $wR2 = 0.1195$, $R1 = 0.0456$. A final difference Fourier map showed no residual density outside -2.42 and 1.43 e $Å^{-3}$, near Pt and I, probably due to residual absorption artefacts. Geometrical calculations were performed with PLATON [19]. All calculations were performed on a DECstation 5000/133. Final coordinates and equivalent isotropic thermal parameters of the non-hydrogen atoms for **3cz** are given in Table 2.

Table 1
Crystal data of **3cz**

Formula	$C_{28}H_{33}N_2PSI_2Pt.CH_2Cl_2$
Molecular weight	1010.44
Crystal system	triclinic
Space group	$P\bar{1}$ (No. 2)
a, b, c (Å)	10.5298(9), 11.5584(8), 14.545(2)
α, β, γ (°)	77.368(8), 84.453(9), 79.720(7)
V (Å^3)	1696.6(3)
Z	2
D_{calc} (g cm^{-3})	1.9778
μ_{calc} (cm^{-1})	62.7 (Mo Kα)
Radiation (Å)	0.71073 (Mo Kα, graphite monochromated)
T (K)	150
Final $R1$ [a]	0.0456
Final $wR2$ [b] [no. data]	0.1195 [7763]
S	1.01

[a] $R1 = \Sigma||F_o| - |F_c||/\Sigma|F_o|$.
[b] $wR2 = [\Sigma[w(F_o^2 - F_c^2)^2]/\Sigma[w(F_o^2)^2]]^{1/2}$.

Table 2
Final coordinates and equivalent isotropic thermal parameters of the non-hydrogen atoms for [Pt(PNS)]I·CH_2Cl_2 (**3cz**)

Atom	x	y	z	U_{eq}
Pt(1)	0.75126(3)	−0.09918(2)	0.20134(2)	0.0210(1)
I(1)	0.73940(5)	−0.18920(4)	0.05556(3)	0.0310(2)
S(1)	0.9769(2)	−0.1361(2)	0.16665(14)	0.0340(6)
P(1)	0.5388(2)	−0.0873(2)	0.23950(12)	0.0216(5)
O(1)	0.7868(6)	0.1519(5)	0.1527(4)	0.0377(19)
N(1)	0.8678(7)	0.2662(6)	0.2329(5)	0.0297(19)
N(2)	0.7696(6)	−0.0247(5)	0.3145(4)	0.0249(17)
C(1)	1.0309(10)	−0.2659(8)	0.2553(7)	0.050(3)
C(2)	1.0516(9)	−0.0239(8)	0.2033(6)	0.038(3)
C(3)	1.0034(8)	−0.0009(7)	0.2992(5)	0.032(2)
C(4)	0.8608(7)	0.0592(6)	0.3060(5)	0.0251(19)
C(5)	0.8311(7)	0.1640(6)	0.2226(5)	0.026(2)
C(6)	0.8599(9)	0.3787(7)	0.1605(6)	0.037(3)
C(7)	0.9334(11)	0.3549(9)	0.0704(7)	0.052(3)
C(8)	0.7186(10)	0.4293(8)	0.1441(8)	0.050(3)
C(9)	0.9242(10)	0.4637(8)	0.1995(7)	0.047(3)
C(10)	0.7104(7)	−0.0505(6)	0.3959(5)	0.0243(19)
C(11)	0.6074(7)	−0.1195(6)	0.4263(5)	0.0231(19)
C(12)	0.5873(8)	−0.1596(7)	0.5238(5)	0.032(3)
C(13)	0.4827(9)	−0.2157(8)	0.5620(6)	0.039(3)
C(14)	0.3945(9)	−0.2313(7)	0.5032(6)	0.036(3)
C(15)	0.4121(8)	−0.1919(7)	0.4063(5)	0.029(2)
C(16)	0.5173(7)	−0.1392(6)	0.3668(5)	0.0216(17)
C(17)	0.4505(7)	−0.1774(7)	0.1894(5)	0.027(2)
C(18)	0.4742(8)	−0.3005(7)	0.2164(6)	0.035(3)
C(19)	0.4150(9)	−0.3698(8)	0.1720(7)	0.042(3)
C(20)	0.3339(9)	−0.3187(9)	0.1013(6)	0.042(3)
C(21)	0.3129(8)	−0.1932(9)	0.0724(5)	0.038(3)
C(22)	0.3719(7)	−0.1229(7)	0.1160(5)	0.030(2)
C(23)	0.4483(7)	0.0635(6)	0.2143(5)	0.0242(19)
C(24)	0.3343(8)	0.0961(7)	0.2627(5)	0.029(2)
C(25)	0.2652(8)	0.2129(7)	0.2415(6)	0.034(2)
C(26)	0.3158(8)	0.2976(7)	0.1729(6)	0.034(2)
C(27)	0.4299(8)	0.2659(7)	0.1245(6)	0.033(2)
C(28)	0.4977(8)	0.1493(7)	0.1440(5)	0.032(2)

2.4. Synthesis of the ligands

2.4.1. N-(N-tert-Butyloxycarbonyl-L-methionine)tert-butylamine (BOC-Met-tBu)

BOC-Met-tBu was prepared following the procedure described for *N*-(*N*-tert-butyloxycarbonyl-*L*-methionine)-histamine (BOC-Met-Histam) [2] using BOC-Met-OH and tert-butylamine. The product was isolated as a white solid in 65% yield. ^{1}H NMR ($CDCl_3$, 293 K, δ): 1.24 (s, 9H, C^7); 1.33 (s, 9H, $(Me)_3C$, BOC); 1.81 (m, 2H, C^3H_2); 1.99 (s, 3H, C^1H_3); 2.45 (m, 2H, C^2H_2); 4.05 (t, H, C^4H). $^{13}C\{^1H\}$ NMR ($CDCl_3$, 293 K, δ): 15.7 (C^1); 28.8 (C^7); 29.1 ($C(Me)_3$, BOC); 30.1 (C^3); 32.3 (C^2); 51.8 (C^6); 54.4 (C^4); 80.3 ($C(Me)_3$, BOC); 156.3 (C^5); 174.0 (C=O, BOC).

The BOC protecting group was removed by HCl, as described for H-Met-Histam·2HCl [2], resulting in HCl·H-Met-tBu. By reacting HCl·L-H-Met-tBu with Et_3N (1.5 equiv.) in EtOH and subsequent evaporation of the solvent, followed by extraction of the obtained white sticky solid with CH_2Cl_2, the racemate *L/D*-H-Met-tBu was collected as a yellow oil in 62% yield. ^{1}H NMR ($CDCl_3$, 293 K, δ): 1.36 (s, 9H, C^7H_3); 2.09 (m, 2H, C^3H_2); 2.12 (s, 3H, C^1H_3); 2.55 (dd, 2H, C^2H_2); 3.88 (t, 1H, C^4H). $^{13}C\{^1H\}$ NMR ($CDCl_3$, 293 K, δ): 14.7 (C^1); 28.3 (C^7); 29.3 (C^3); 31.9 (C^2); 52.0 (C^6); 53.5 (C^4); 157.1 (C^5).

2.4.2. N-[N-{2-(Diphenylphosphino)benzylidene}-3-propylethylsulfide] (PNS-1, a); N-[N-{2-(diphenylphosphino)benzylidene}-L-methioninol] (PNS-2, b); N-[N-{2-(diphenylphosphino)benzylidene}-D/L-methionyl]-tert-butylamine (PNS-3, c)

Employing the method described for 2-(diphenylphosphino)-benzylidene-*R*(±)-α-methyl-benzylamine [20] and using H-Met-tBu and 2-(diphenylphosphino)-benzaldehyde afforded ligand **c** in 72% yield, as a yellow oil. **c**: IR (CH_2Cl_2, cm^{-1}): 1631 (C=N); 1650 (C(O)NH). $^{13}C\{^1H\}$ NMR ($CDCl_3$, 293 K, δ): 14.5 (C^1); 28.8 (C^7); 29.3 (C^3); 33.1 (C^2); 51.2 (C^6); 73.3 (C^4); 161.7 (C^{10}); 171.6 (C^5). **a**: $^{13}C\{^1H\}$ NMR ($CDCl_3$, 293 K, δ): 15.3 (S–CH_2CH_3); 26.3 (S-CH_2CH_3); 29.6 (N–$CH_2CH_2CH_2$); 32.9 (N–$CH_2CH_2CH_2$); 59.2 (N–$CH_2CH_2CH_2$). **b**: $^{13}C\{^1H\}$ NMR ($CDCl_3$, 293 K, δ): 15.9 (C^1); 30.6 (C^3); 31.8 (C^2); 66.7 (C^5); 71.7 (C^4); 161.3 (C^{10}). Elemental analyses failed due to traces of amine, but from the spectroscopic details there is no doubt about the composition of the ligand.

2.4.3. N-[N-{2-(Pyridine)methylidene}-D/L-methionyl]-tert-butylamine (NN'S, d)

The preparation was similar to the PNS ligands using 2-pyridine carboxaldehyde. **d**: $^{13}C\{^1H\}$ NMR ($CDCl_3$, 293 K, δ): 15.5 (C^1); 29.2 ($C^{7,8,9}$); 30.4 (C^3); 34.3 (C^2); 51.3 (C^6); 73.0 (C^4); 121.9 (C^{13}); 125.9 (C^{12}); 137.2 (C^{14}); 150.3 (C^{15}); 154.1 (C^{11}) 164.3 (C^{10}); 171.6 (C^5). ^{15}N NMR ($CDCl_3$, 293 K, δ): −47.6 (pyridyl-N); −34.8 (imine-N). Elemental analysis failed due to traces of polymerized 2-pyridine carboxaldehyde and the instability of the ligand, leading to the starting compounds H-Met-tBu and the aldehyde.

2.5. Synthesis of the complexes

2.5.1. [MCl(L)]Cl (L = PNS-2, M = Pd (1by); L = PNS-3, M = Pd (1cy), Pt (1cz); L = NN'S, M = Pd (1dy))

To a stirred suspension of $[PdCl_2(COD)]$ (0.21 g; 0.72 mmol) in CH_2Cl_2 (10 ml), a solution of the PNS-3 ligand (0.46 g; 0.72 mmol) in CH_2Cl_2 (15 ml) was added. The mixture was stirred for 18 h at room temperature, after which the solvent was evaporated. The resulting off-white sticky solid was washed with Et_2O (2×10 ml) and subsequently dried, which afforded an air stable solid in 95% yield. *Anal.* Found: C, 51.39; H, 5.13; N, 4.26. Calc. for $C_{28}H_{33}N_2OPSCl_2Pd$: C, 51.43; H, 5.09; N, 4.28%. **1cy**: IR (CH_2Cl_2, cm^{-1}): 1610 (C=N); 1652 (C(O)NH). $^{13}C\{^1H\}$ NMR ($CDCl_3$, 293 K, δ): 22.1 (C^1); 28.7 ($C^{7,8,9}$); 33.9 (broad, C^3); 34.7 (broad, C^2); 55.4 (C^6); 166.4 (broad, C^{10}); 176.8 (C^5); C^4 obscured by $CDCl_3$. Complex **1cy** showed a specific conductivity of $\Delta = 356\ \Omega^{-1}\ cm^2\ mol^{-1}$ (CH_2Cl_2, 223 K); $\Delta = 703\ \Omega^{-1}\ cm^2\ mol^{-1}$ (CH_2Cl_2, 293 K); $\Delta = 797\ \Omega^{-1}\ cm^2\ mol^{-1}$ (CH_2Cl_2, 323 K).

1by, **1dy** and **1cz** were synthesized similar to **1cy**, using $[PtCl_2(COD)]$ (0.12 g; 0.32 mmol) in CH_2Cl_2 (10 ml). **1cz**: $^{13}C\{^1H\}$ NMR ($CDCl_3$, 293 K, δ): 16.4 (C^1); 28.1 ($C^{7,8,9}$); 30.7 (C^3); 34.4 (C^2); 53.8 (C^6); 163.8 (C^{10}); C^4 is obscured by $CDCl_3$ while C^5 is not observed. Because of the similarity of the products with **1cy** no elemental analyses were carried out.

2.5.2. [PdBr(L)]Br (L = PNS-3 (2cy), NN'S (2dy))

$PdBr_2$ (0.91g; 3.39 mmol) was suspended in a mixture of CH_2Cl_2 (15 ml) and MeCN (10 ml) followed by addition of a PNS ligand solution in CH_2Cl_2 (13.2 ml of 0.26 M). The resulting purple suspension was stirred for at least 18 h at room temperature during which period the color of the mixture slowly changed to red. The red mixture was filtered and subsequently reduced to 5 ml by evaporation, after which Et_2O (20 ml) was added which caused a yellow solid to precipitate. Complex **2cy** was isolated in quantitative yield by filtration and subsequently dried in vacuo. *Anal.* Found: C, 45.17; H, 4.52; N, 3.79. Calc. for $C_{28}H_{33}N_2OPSBr_2Pd$: C, 45.27; H, 4.48; N, 3.77%. **2cy**. IR (CH_2Cl_2, cm^{-1}): 1612 (C=N); 1648 (C(O)NH). $^{13}C\{^1H\}$ NMR ($CDCl_3$, 293 K, δ): 15.5 (C^1); 28.6 ($C^{7,8,9}$); 29.9 (C^3); 34.8 (C^2); 53.9 (C^6); 78.4 (C^4); 165.4 (C^{10}); 174.0 (C^5). Complex **2cy** showed a specific conductivity of $\Delta = 367\ \Omega^{-1}\ cm^2\ mol^{-1}$ (CH_2Cl_2, 223 K); $\Delta = 689\ \Omega^{-1}\ cm^2\ mol^{-1}$ (CH_2Cl_2, 293 K); $\Delta = 943\ \Omega^{-1}\ cm^2\ mol^{-1}$ (CH_2Cl_2, 323 K).

Complex **2dy** was synthesized similar to **2cy**, using $PdBr_2$ (0.09 g; 0.32 mmol). **2dy**: $^{13}C\{^1H\}$ NMR ($CDCl_3$, 293 K, δ): 15.8 (C^1); 29.3 ($C^{7,8,9}$); 32.2 (C^3); 32.8 (C^2); 53.1 (C^6); 64.6 (broad, C^4); 129.8 (C^{13}); 130.4 (C^{12}); 141.8 (C^{14}); 153.1 (C^{15}); 154.8 (C^{11}); 167.8 (C^5); 174.4 (C^{10}).

Elemental analysis was not performed due to the similarity of the product with **1cy**.

2.5.3. [PtI(L)]I (L = PNS-3 (3cz), NN'S (3dz))

3cz and **3dz** were prepared similarly to **1cy** using [PtI_2(COD)] (0.28 g; 0.50 mmol) in CH_2Cl_2 (10 ml). Slow diffusion of Et_2O into a concentrated solution of **3cz** in CH_2Cl_2 afforded yellow crystals. *Anal.* Found: C, 36.42; H, 3.68; N, 2.92. Calc. for $C_{28}H_{33}N_2OPSI_2Pt$: C, 36.34; H, 3.60; N, 3.03%. **3cz**: IR (CH_2Cl_2, cm^{-1}): 1612 (C=N); 1647 (C(O)NH). $^{13}C\{^1H\}$ NMR ($CDCl_3$, 293 K, δ): 19.2 (broad, C^1); 29.0 ($C^{7,8,9}$); 29.3 (C^3); 33.9 (broad, C^2); 54.7 (C^6); 75.3 (broad, C^4); 163.6 (broad triplet, $^3J_{Pt-C}$ = 44 Hz, C^{10}). Complex **3c** showed a specific conductivity of $\Delta = 569\ \Omega^{-1}$ cm^2 mol^{-1} (CH_2Cl_2, 223 K); $\Delta = 992\ \Omega^{-1}$ cm^2 mol^{-1} (CH_2Cl_2, 293 K); $\Delta = 1106\ \Omega^{-1}$ cm^2 mol^{-1} (CH_2Cl_2, 323 K).

2.5.4. [M(Me)(L)]Cl (L = PNS-1, M = Pd (4ay), M = Pt (4az); L = PNS-2, M = Pd (4by), M = Pt (4bz); L = PNS-3, M = Pd (4cy); L = NN'S, M = Pd (4dy))

The complexes were prepared similar to **1cy**, using [PdCl(Me)(COD)] (0.59 g; 2.33 mmol) in CH_2Cl_2 (5 ml). **4cy**: *Anal.* Found: C, 54.92; H, 5.69; N 4.49. Calc. for $C_{29}H_{36}N_2OPSClPd$: C, 54.98; H, 5.73; N, 4.42%. **4cy**: IR (CH_2Cl_2, cm^{-1}): 1614 (C=N); 1656 (C(O)NH). $^{13}C\{^1H\}$ NMR ($CDCl_3$, 293 K, δ): 0.1 (broad, Pd–Me); 27 (broad, $C^{7,8,9}$); 163.1 (broad, C^{10}); the resonances of C^1, C^2, C^3, C^4, C^6 were very broad and could therefore not be properly assigned. Complex **4cy** showed a specific conductivity of $\Delta = 530\ \Omega^{-1}$ cm^2 mol^{-1} (CH_2Cl_2, 223 K); $\Delta = 941\ \Omega^{-1}$ cm^2 mol^{-1} (CH_2Cl_2, 293 K); $\Delta = 1208\ \Omega^{-1}$ cm^2 mol^{-1} (CH_2Cl_2, 323 K).

4bz: $^{13}C\{^1H\}$ NMR ($CDCl_3$, 293 K, δ): −12.9 (J_{Pt-C} = 622 Hz, J_{P-C} = 5.3 Hz, Pt–Me); 15.9 (J_{Pt-C} = 26.2 Hz, C^1); 28.8 (C^3); 32.6 (J_{Pt-C} = 27.4 Hz, C^2); 66.4 (C^5); 72.9 (broad, C^4); 165.1 (broad, C^{10}). **4dy**: $^{13}C\{^1H\}$ NMR ($CDCl_3$, 293 K, δ): 3.8 (Pd–Me); 22.3 (C^1); 29.1 ($C^{7,8,9}$); 29.3 (C^3); 31.3 (C^2); 52.4 (C^6); 66.2 (C^4); 129.0 (C^{13}); 129.5 (C^{12}); 141.3 (C^{14}); 148.5 (C^{15}); 155.4 (C^{11}); 167.7 (C^{10}); 169.0 (C^5). ^{15}N NMR ($CDCl_3$, 293 K, δ): −139.8 (pyridyl-N); −70.2 (imine-N). As **4ay**, **4az**, **4by**, **4bz** and **4dy** are analogous to **4cy** no elemental analysis was performed.

2.5.5. [Pd(Me)(L)]Br (L = PNS-3 (5cy), NN'S (5dy))

To a solution of **7cy** (0.81 g; 1.08 mmol) in CH_2Cl_2 (15 ml), $Ag(O_3SCF_3)$ (0.29 g; 1.14 mmol) was added. The resulting solution was stirred for 18 h at room temperature, which caused a color change to yellow. After filtration and subsequent evaporation of the solvent a yellow solid was obtained in 93% yield. *Anal.* Found: C, 51.52; H, 4.88; N, 4.11. Calc. for $C_{29}H_{36}N_2OPSBrPd$: C, 51.61; H, 4.93; N, 4.15%. **5cy**: IR (CH_2Cl_2, cm^{-1}): 1611 (C=N); 1655 (C(O)NH). $^{13}C\{^1H\}$ NMR ($CDCl_3$, 293 K, δ): 2.8 (Pd–Me); 19.6 (C^1); 28.7 ($C^{7,8,9}$); 32.3 (broad, C^3); 34.8 (broad, C^2); 54.0 (C^6); 72.4 (C^4); 164.9 (C^{10}); 176.9 (C^5). Complex **5cy** showed a specific conductivity of $\Delta = 523\ \Omega^{-1}$ cm^2 mol^{-1} (CH_2Cl_2, 223 K); $\Delta = 873\ \Omega^{-1}$ cm^2 mol^{-1} (CH_2Cl_2, 293 K); $\Delta = 996\ \Omega^{-1}$ cm^2 mol^{-1} (CH_2Cl_2, 323 K).

Complex **5dy** was prepared similarly to **5cy**. $^{13}C\{^1H\}$ NMR ($CDCl_3$, 293 K, δ): 3.2 (Pd–Me); 21.9 (C^1); 29.2 ($C^{7,8,9}$); 29.8 (C^3); 32.0 (C^2); 52.2 (C^4); 66.4 (C^6); 128.9 (C^{13}); 129.8 (C^{12}); 141.5 (C^{14}); 148.3 (C^{15}); 154.8 (C^{11}); 167.5 (C^{10}); 171.2 (C^5). As **5dy** is analogous to **5cy** no elemental analysis was performed.

2.5.6. [Pd(Me)(PNS-3)]I (6cy)

To a solution of **4cy** (0.09 g; 0.15 mmol) in CH_2Cl_2 (10 ml) NH_4I (excess) was added. The color of the solution turned red within 2 min. After 10 min the solution was filtered and the solvent was subsequently evaporated, resulting in a hygroscopic red solid **6cy** in 84% yield. **6cy**: IR (CH_2Cl_2, cm^{-1}): 1608 (C=N); 1656 (C(O)NH). $^{13}C\{^1H\}$ NMR ($CDCl_3$, 293 K): 1.3 (broad, Pd–Me); 15.0 (C^1); 28.7 ($C^{7,8,9}$); 30.4 (broad, C^3); 32.7 (broad, C^2); 51.3 (C^6); 72.3 (C^4); 165.5 (broad, C^{10}); C^5 is not observed. Complex **6cy** showed a specific conductivity of $\Delta = 498\ \Omega^{-1}$ cm^2 mol^{-1} (CH_2Cl_2, 223 K); $\Delta = 872\ \Omega^{-1}$ cm^2 mol^{-1} (CH_2Cl_2, 293 K); $\Delta = 1062\ \Omega^{-1}$ cm^2 mol^{-1} (CH_2Cl_2, 323 K). Elemental analysis failed due to the presence of a small amount of NH_4I, which could not be avoided.

2.5.7. [M(Me)(L)](O$_3$SCF$_3$) (L = PNS-1, M = Pd (7ay), M = Pt (7az); L = PNS-2, M = Pd (7by); L = PNS-3, M = Pd (7cy); L = NN'S, M = Pd (7dy))

To a solution of **4cy** (0.16 g; 0.26 mmol) in $CDCl_3$ (10 ml) $Ag(O_3SCF_3)$ (0.07 g; 0.27 mmol) was added. After 5 min the resulting suspension was filtered resulting in a clear solution of **7cy**. **7cy**: IR (CH_2Cl_2, cm^{-1}): 1607 (C=N); 1653 (C(O)NH). $^{13}C\{^1H\}$ NMR ($CDCl_3$, 293 K, δ): 7 (broad, Pd–Me); 14.9 (C^1); 26.6 ($C^{7,8,9}$); 28.6 (C^3); 31.4 (C^2); 50.2 (C^6); 69.5 (C^4); 163.3 (C^{10}); 168.4 (C^5). Complex **7cy** showed a specific conductivity of $\Delta = 623\ \Omega^{-1}$ cm^2 mol^{-1} (CH_2Cl_2, 223 K); $\Delta = 1021\ \Omega^{-1}$ cm^2 mol^{-1} (CH_2Cl_2, 293 K); $\Delta = 1475\ \Omega^{-1}$ cm^2 mol^{-1} (CH_2Cl_2, 323 K).

Complexes **7ay**, **7az**, **7by** and **7dy** were prepared similarly to **7cy**, using **4ay**, **4az**, **4by** and **4dy**, respectively. Elemental analysis of **7ay**, **7az**, **7by**, **7cy** and **7dy** could not be carried out due to slow degradation of the solid product, with formation of colloidal palladium or platinum. **7dy**: ^{15}N NMR ($CDCl_3$, 293 K, δ): −158.0 (pyridyl-N); −71.1 (imine-N).

2.5.8. [Pd(CH$_2$C(Me)C(R)$_2$)(PNS)]Cl (R = H (8cy), Me (9cy))

To a stirred solution of [(PdCl(η^3-$CH_2C(Me)CH_2$))$_2$] (0.07 g; 0.18 mmol) in CH_2Cl_2 (4 ml) at room temperature a solution of L (0.23 g; 0.36 mmol) in CH_2Cl_2 (3 ml) was added. The mixture was stirred for 1 h after which the solvent was removed in vacuo, yielding **8cy** as a yellow solid. **8cy**,

major component: $^{13}C\{^1H\}$ NMR ($CDCl_3$, 293 K, δ): 14.5 (broad, C^1); 19.1, 19.4 ($C^{2\prime}Me$); 26.8 ($C^{7,8,9}$); 31.4 (C^3); 33.3 (C^2); 49.1 ($C^{1\prime}H_2$); 49.3 (C^6); 51.9 ($C^{3\prime}H_2$); 70.9 (broad, C^4); 119.7 (broad, $C^{2\prime}$), 159.5 (C^{10}); 169.4 (broad, C^5). **8cy**, minor component: $^{13}C\{^1H\}$ NMR ($CDCl_3$, 293 K, δ): 15.1 (C^1); 20.8 ($C^{2\prime}Me$); 26.5 ($C^{7,8,9}$); 29.0 (broad, C^2 and C^3); 33.4 ($C^{1\prime}$); 69.2 (broad, C^4); 105.5 ($C^{3\prime}$); 120.0 (broad, $C^{2\prime}$); 163.0 (C^{10}); 172.2 (broad, C^5). Complex **8cy** showed a specific conductivity of $\Delta = 764\ \Omega^{-1}\ cm^2\ mol^{-1}$ (CH_2Cl_2, 223 K); $\Delta = 945\ \Omega^{-1}\ cm^2\ mol^{-1}$ (CH_2Cl_2, 293 K); $\Delta = 1153\ \Omega^{-1}\ cm^2\ mol^{-1}$ (CH_2Cl_2, 323 K).

9cy: $^{13}C\{^1H\}$ NMR ($CDCl_3$, 293 K, δ): 16.4 (broad, C^1); 22.1 (Me^a); 22.6 ($C^{2\prime}Me$); 27.4 (Me^s); 27.6 ($C^{7,8,9}$); 27.9 (Me^s); 30.2 (broad, C^3); 32.2 (broad, C^2); 50.0 (C^6); 50.7 (broad, $C^{3\prime}H_2$); 71.7 (broad, C^4); 109.5 ($C^{2\prime}$); 167.0 (broad, C^{10}); 167.7 (broad, C^5); 170.2 ($C^{1\prime}Me_2$).

Elemental analysis of **8cy** and **9cy** could not be carried out due to the presence of small amounts of $[(PdCl(\eta^3\text{-}CH_2C(Me)CH_2)]_2$, which could not be removed.

2.5.9. [Pd(CH$_2$C(Me)C(R)$_2$)(PNS)](O$_3$SCF$_3$) (R = H (10cy), Me (11cy))

To a stirred solution of **8cy** (0.18 g; 0.21 mmol) in $CDCl_3$ (5 ml) $Ag(O_3SCF_3)$ (0.05 g; 0.22 mmol) was added, resulting in the formation of a white precipitate, which was filtered off, yielding a yellow solution of **10cy** in $CDCl_3$. $^{13}C\{^1H\}$ NMR ($CDCl_3$, 293 K, δ): 14.2 (C^1); 21.6 ($C^{2\prime}Me$); 27.1 ($C^{7,8,9}$); 30.6 (C^3); 33.7 (C^2); 50.1 (C^6); 51.8 (broad, $C^{1\prime}H_2$); 53.8 (broad, $C^{3\prime}H_2$); obscured (C^4); 115.1 ($C^{2\prime}$); 163.2 (broad, C^{10}); 171.2 (broad, C^5). Complex **10cy** showed a specific conductivity of $\Delta = 803\ \Omega^{-1}\ cm^2\ mol^{-1}$ (CH_2Cl_2, 223 K); $\Delta = 934\ \Omega^{-1}\ cm^2\ mol^{-1}$ (CH_2Cl_2, 293 K); $\Delta = 1067\ \Omega^{-1}\ cm^2\ mol^{-1}$ (CH_2Cl_2, 323 K).

11cy: $^{13}C\{^1H\}$ NMR ($CDCl_3$, 293 K, δ): 15.5 (broad, C^1); 20.6 ($C^{2\prime}Me$); 22.9 (Me^a); 24.4 ($C^{7,8,9}$); 27.6 (Me^s); 29.9 (broad, C^3); 31.8 (broad, C^2); 52.0 ($C^{1\prime}H_2$); 52.2 (C^6); 55.0 ($C^{3\prime}H_2$); 73.3 (C^4); 118.5 ($C^{2\prime}$); 167.9 (broad, C^{10}); 176.1 (C^5). Elemental analysis of **10cy** and **11cy** could not be carried out due to degradation of the solid product, with formation of colloidal palladium or platinum.

2.5.10. [M(COMe)(L)]X (M = Pd: L = PNS-1, X = Cl (12ay); L = PNS-2, X = Cl (12by); L = PNS-3, X = Cl (12cy), X = Br (13cy), X = I (14cy), X = O$_3$SCF$_3$ (15cy); L = NN'S, X = Cl (12dy), X = O$_3$SCF$_3$ (15dy); M = Pt: L = PNS-2, X = Cl (12bz))

In a typical experiment complex **4cy** (approximately 0.15 mmol) in $CDCl_3$ (1.5 ml) was pressurized with CO (10 bar) at room temperature in a high-pressure 10 mm NMR tube. **12cy**: IR (CH_2Cl_2, cm^{-1}): 1702 (Pd–C(O)Me); 1610 (C=N); 1652 (C(O)NH). **12cy**: $^{13}C\{^1H\}$ NMR ($CDCl_3$, 293 K, δ): 16.5 (C^1); 28.9 ($C^{7,8,9}$); 30.9 (C^3); 33.5 (C^2); 39.4 (Pd–C(O)*Me*); 52.1 (C^6); 68.7 (C^4); 167.2 (C^{10}); 168.4 (C^5). **13cy**: IR (CH_2Cl_2, cm^{-1}): 1704 (Pd–C(O)Me); 1611 (C=N); 1655 (C(O)NH). **14cy**: IR (CH_2Cl_2, cm^{-1}): 1699 (Pd–C(O)Me); 1614 (C=N); 1648 (C(O)NH). **15cy**: IR (CH_2Cl_2, cm^{-1}): 1705 (Pd–C(O)Me); 1612 (C=N); 1653 (C(O)NH). Elemental analysis could not be performed due to decarbonylation upon release of CO pressure, which is accompanied by gradual degradation of the product with formation of colloidal palladium.

3. Results

In earlier studies it was found that upon condensation of a methionine methyl ester residue with a phosphorus functionalized aldehyde the product is instable and hydrolysis of the imine bond takes place. In order to stabilize the imine bond the methionine was protected as an amide. The first step in the PNS-3 and NN'S ligand synthesis involves the formation of the optically active BOC protected methionine, which is subsequently coupled with H_2N-*t*Bu (Scheme 1, Eqs. (1) and (2)). Reaction of this enantio-pure BOC-*L*-met-tBu with HCl in order to remove the protecting group and subsequent reaction with Et_3N resulted in the abstraction of HCl of the HCl · Hmet-tBu intermediate and in racemization of the chiral carbon atom of the amino acid moiety, i.e. of C(4)H (Scheme 1, Eq. (3)). The non-substituted $H_2N\text{-}(CH_2)_3\text{-}S\text{-}Et$ was made by reaction of bromopropyl-phthalimide with EtSH and subsequent removal of the protecting group by reaction with HCl (Eq. (6)). The PNS-1 (**a**), PNS-2 (**b**), PNS-3 (**c**) and NN'S (**d**) ligands were prepared by reacting the proper amine, i.e. H_2N-Prop-S-Et (**a**), methioninol (**b**, commercially available) and Hmet-*t*Bu (**c** and **d**), with 2-(diphenylphosphino)-benzylidene and 2-pyridine-carbaldehyde (Eqs. (4) and (5)).

The yellow bidentate PNS ligands all show phosphorus coupling on the imine proton of the free ligand in ^1H NMR (4.7 Hz in PNS-1, 3.9 Hz in PNS-2 and 2.9 Hz in PNS-3), which points to a through-space coupling [21], indicating that the imine H atom (C(10)H) is directed towards the lone pair of the phosphorus atom.

The bischloride complexes [PdCl(L)]Cl (**1**) were prepared by reaction of $[PdCl_2(COD)]$ with **b**, **c** and **d**, while the corresponding platinum complex was only prepared with **c** (Scheme 2). [PdBr(L)]Br (**2**) complexes were synthe-

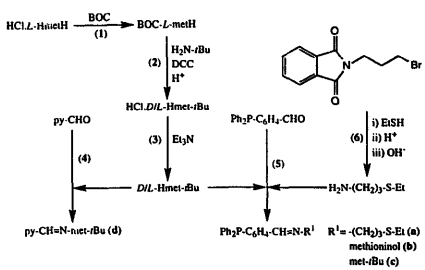

Scheme 1. Formation of the ligands.

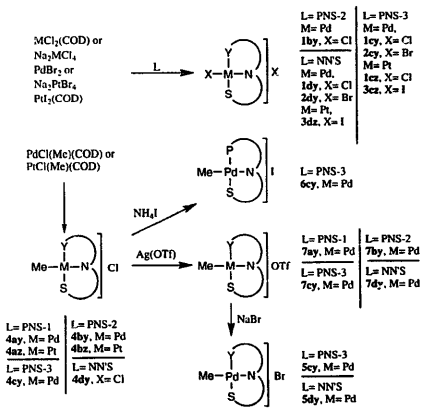

Scheme 2. Numbering of the starting complexes and products.

sized by reaction of $PdBr_2$ with **c** and **d**, whereas the iodide-platinum analogue (**3**) was synthesized using $[PtI_2(COD)]$ in combination with **c** and **d**.

The methyl complexes [Pd(Me)(L)]Cl (**4**) were prepared by reaction of **a**, **b**, **c** and **d** with [PdCl(Me)(COD)], while the corresponding platinum analogue was prepared from [PtCl(Me)(COD)] using only ligands **a** and **b**. The methyl-iodide complex (**6**) containing **c** was prepared by reacting [Pd(Me)(PNS-3)]Cl with NH_4I. The [Pd(Me)-(L)](O_3SCF_3) complexes (**7**, L = **a**, **b**, **c** and **d**) were formed by abstracting the halide ligand from [Pd(Me)(L)]Cl with $Ag(O_3SCF_3)$ (Scheme 2). The [Pd(Me)(L)]Br complexes (**5**, L = **c** and **d**) were obtained by reacting **7** with NaBr. The palladium compounds are labeled **y**, while the corresponding platinum complexes are labeled **z**.

The bis-halide (**1**, **2** and **3**) and methyl-halide (**4**, **5** and **6**) complexes dissolve in polar solvents and can be stored in the open air for a prolonged period. Heating solutions of these complexes in CH_2Cl_2 or $CDCl_3$ ($T > 363$ K, 18 h) caused slow decomposition as shown by the formation of traces of colloidal palladium or platinum. The complexes with $X = O_3SCF_3^-$ (**7**) are hygroscopic and instable and were therefore prepared in situ.

3.1. [MX(L)]X (X = Cl, Br, I); [M(Me)(L)]X (X = Cl, Br, I, OTf)

The molecular structure of [PtI(PNS-3)]I·CH_2Cl_2 (**3cz**) in the solid state (Fig. 2) shows the expected square planar coordination around the metal center formed by the P (Pt–P(1) = 2.240(2) Å), imine-N (Pt–N(2) = 2.056(6) Å) and the S (Pt–S(1) = 2.363(2) Å) donor atoms of the PNS ligand and an iodide ligand (Pt–I(1) = 2.5801(6) Å), while the second iodide is not bonded to the metal center, as indicated by the Pt–I(2) distance of 5.5342(10) Å. The ionic iodide atom is connected by hydrogen bonds with the amide hydrogen and with the solvent hydrogen atoms, as indicated by the H(100)···I(2), H(29A)···I(2) and H(29B)···I(2) distances of 3.674(7), 3.911(11) and 3.868(5) Å, respectively. All distances (Table 3) are in the expected range [22]. The six-membered NS containing chelate ring has a chair conformation, similar to the conformation found for methionine platinum and palladium complexes [$PtCl_2$(*L*-MetH-*S,N*)], [$PtCl_2$(*L*/*D*-MetH-*S,N*)] [7] and [$PdCl_2$(*L*/*D*-

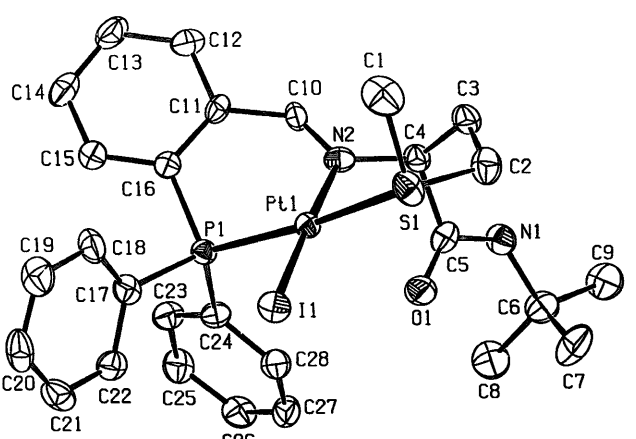

Fig. 2. Molecular structure of **3cz** in the solid state.

Table 3
Selected distances (Å) and angles (°) for **3cz** (e.s.d.s in parentheses)

Pt–I(1)	2.5801(6)	C(10)–C(11)–C(16)–P(1)	6.4(10)
Pt–P(1)	2.240(2)	N(2)–C(10)–C(11)–C(16)	−24.0(13)
Pt–S(1)	2.363(2)	Pt(1)–N(2)–C(10)–C(11)	−9.9(11)
Pt–N(2)	2.056(6)	P(1)–Pt(1)–N(2)–C(10)	40.4(6)
H(100)···I(2)	3.674(7)	N(2)–Pt(1)–P(1)–C(16)	−44.4(3)
H(29A)···I(2)	3.911(11)	Pt(1)–P(1)–C(16)–C(11)	32.0(6)
H(29B)···I(2)	3.868(5)	Pt(1)–N(2)–C(4)–C(3)	−68.9(7)
		C(2)–C(3)–C(4)–N(2)	79.3(8)
I(1)–Pt–S(1)	84.19(5)	S(1)–C(2)–C(3)–C(4)	−67.0(8)
S(1)–Pt–N(2)	93.17(19)	Pt(1)–S(1)–C(2)–C(3)	44.9(7)
N(2)–Pt–P(1)	89.14(19)	N(2)–Pt(1)–S(1)–C(2)	−29.4(3)
P(1)–Pt–I(1)	93.63(5)	S(1)–Pt(1)–N(2)–C(4)	43.2(5)

MetH-*S,N*)] [8]. By comparison with the C(4)–C(3)–C(2)–S and N–C(4)–C(3)–C(2) dihedral angles of −67.0(8) and 79.3(8)° of **3cz** with the analogous values found for the *N*-[*N*-(5-methyl-2-thienylmethylidene)-*L*-methionyl]histamine ligand [2] (170.0(2) and 178.8(3)°, respectively), one may infer that a rotation is needed of the methionine side arm in order to bind the PNS-3 ligand also as an NS chelate. The coordination fashion is therefore controlled by the metal and not by the ligand, as is the case for *N*-[*N*-(5-methyl-2-thienylmethylidene)-*L*-methionyl]-histamine [2,3]. The six-membered PN chelate ring shows a perturbed envelope conformation, as indicated by the dihedral angles of 6.4(10)° for C10–C11–C16–P1 and 32.0(6)° for the Pt1–P1–C16–C11 units, respectively, similar to the conformation found for the bis-chloridepalladium complex with 2-(diphenylphosphino)benzylidene-*S*(−)-α-methylbenzylamine [20]. Both the methyl group on the sulfur donor, i.e. C(1), and the C(O)NH-tBu moiety are positioned quasi-axial with respect to the NS chelate ring, thus giving the sulfur atom an *R* configuration, and C(4) an *S* configuration.

The coordination fashion of the PNS ligands could be ascertained by using the phosphorus donor atom, the imine proton (C(10)H) and the alkyl substituent on the sulfur donor (C(1)) as probes in $^{31}P\{^1H\}$, ^1H and $^{13}C\{^1H\}$ NMR, respectively.

Phosphorus coordination is clear from the downfield shift of the $^{31}P\{^1H\}$ NMR resonance signal (Table 4), compared to the free ligand, which is approximately 40 ppm for the bis-halide (**1by**, **1cy** and **2cy**) and 50 ppm for the methyl-halide palladium complexes (**4ay**, **7ay**, **4by**, **7by**, **4cy–7cy**). The platinum complexes show a smaller downfield shift, i.e. 10 ppm for the bis-halide platinum compounds (**1cz** and **3cz**) and 30 ppm for the methyl-halide platinum complexes (**4az** and **4bz**). Platinum–phosphorus coupling (Table 4) further illustrates phosphorus coordination.

Imine nitrogen coordination of the bis-halide complexes (**1by**, **1cy**, **1cz**, **2cy** and **3cz**) is inferred from the downfield shift of the imine proton (C(10)H) of approximately 0.6 ppm, which is accompanied by the disappearance of the through-space phosphorous–imine proton coupling, indicating a rotation of the C11–C10 bond as is needed for chelate bonding. The methyl-halide complexes (**4ay**, **7ay**, **4by**, **7by**, **4cy-7cy**) also show a ^1H shift of C(10)H, which is both a downfield (**4by**, **4cy–7cy**) as well as an upfield (**4ay**, **7ay** and **7by**) shift, again indicating nitrogen coordination. Terdentate coordination of the PNS ligands in solution of both the bis-halide as well as the methyl-halide complexes is further illustrated by the downfield shift of the S–Me group ($C(1)H_3$) of approximately 0.3 ppm (Table 4).

Coordination of the nitrogen and sulfur atoms is also supported by the downfield shifts of C(1) ($0.4 < \Delta\delta < 7.6$ ppm) and C(10) ($1.4 < \Delta\delta < 4.7$ ppm) in the $^{13}C\{^1H\}$ NMR spectrum of **1cy–6cy** (Section 2) when compared to those values found for the free ligand.

The platinum imine proton (C(10)H) coupling of 82, 53 and 43 Hz observed for **1cz**, **3cz** and **4bz**, respectively, further demonstrates imine coordination, while the latter complex also shows a carbon platinum coupling of 27 Hz on C(2) indicating sulfur coordination (Section 2). This coupling could unfortunately not be observed for complexes **1cz** and **3cz**.

Conductivity experiments (Section 2) measured for the complexes containing the PNS-3 ligand (**1cy–7cy**) clearly indicate the existence of ionic species in CH_2Cl_2 thereby indicating again that terdentate coordination is dominant for all the complexes containing the PNS-3 ligand. These findings are also supported by an osmometry molecular weight measurement for **4cy** at 313 K, which yielded an average molecular weight of $M_w = 303 \pm 10$. This value is almost half of the calculated mass of [Pd(Me)(PNS-3)]Cl ($M_c = 633.5$), which is to be expected for a dissociated [Pd(Me)(PNS-3)]Cl complex.

Coordination of both nitrogen donor atoms of the NN'S ligand (**d**) could easily be determined by the large upfield shifts of both the pyridyl ($\Delta\delta = 92.2$ ppm for **4dy** and $\Delta\delta = 110.4$ ppm for **7dy**) and imine nitrogen ($\Delta\delta = 35.4$ ppm for **4dy** and $\Delta\delta = 36.3$ ppm for **7dy**) atoms in $^{15}N\{^1H\}$ NMR (Section 2), as has also been observed for terdentate nitrogen palladium complexes [23].

Terdentate coordination of the NN'S ligand in the palladium complexes **1dy**, **2dy**, **4dy** and **5dy** is further illustrated by the ^1H downfield shifts of C(10)H, $C(1)H_3$ and C(15)H, being approximately 0.7–1.6, 0.5–0.8 and 0.4–0.8 ppm,

Table 4
$^{31}P\{^1H\}$ and relevant ^1H NMR of the PNS-1 (**a**), PNS-2 (**b**), PNS-3 (**c**) and NN'S (**d**) containing complexes, measured at 293 K in $CDCl_3$

	$^{31}P\{^1H\}$	$C^{10}H$	$CH_2C^1H_3$	C^4H	Pd–Me	Pd–C(O)Me
PNS-1 (**a**)	−12.9	8.90{4.7}	1.2–2.2	3.6[w]		
[Pd(Me)]Cl (**4ay**)	37.5[s]	8.28[s]	1.9–2.4[b]	4.29[b]	0.57[b]	
[Pt(Me)]Cl (**4az**)	18.6[3967]	9.44[b]	2.2–2.6[b]	4.23[b]	0.14[bx][63]	
[Pd(Me)]OTf (**7ay**)	41.6[s]	8.57	1.8–2.3[b]	5.50[b]	0.32[s]	
[Pd(C(O)Me)]Cl (**12ay**)	19.4[s]	8.20[s]	2.0–2.4[b]	4.29[b]		2.37[s]
	$^{31}P\{^1H\}$	$C^{10}H$	C^1H_3	C^4H	M–Me	M–C(O)Me
PNS-2 (**b**)	−9.41	8.74{3.9}	1.99[s]	3.40[s]		
[PdCl]Cl (**1by**)	32.7[s]	9.17[s]	2.29[s]	3.87[t]		
[Pd(Me)]Cl (**4by**)	35.8[s]	9.08[s]	2.32[s]	3.88[b]	0.52[s]	
[Pt(Me)]Cl (**4bz**)	20.0[3986]	8.98[42.6]	2.33[w]	3.91[b]	0.25{4.2}[70]	
[Pd(Me)]OTf (**7by**)	39.6[s]	8.53[s]	2.34[s]	3.92[t]	0.38{2.5}	
[Pd(C(O)Me)]Cl (**12by**)	18.6[s]	8.24[s]	2.21[b]	3.89[b]		2.38[s]
[Pt(C(O)Me)]Cl (**12bz**)	10.9[4011]	8.99[40.0]	2.19[b]	3.96[b]		2.40[s]
PNS-3 (**c**)	−7.8[s]	8.44[d]{2.9}	1.97[s]	3.48[y]		
[PdCl]Cl (**1cy**)	35.9[s]	9.01[s]	2.18[b]	6.01[b]		
[PtCl]Cl (**1cz**)	2.3[3883]	8.73[t][82]	2.33[s]	6.33[b]		
[PdBr]Br (**2cy**)	39.9[s]	9.43[s]	2.22[s]	6.18[b]		
[PtI]I (**3cz**)	4.5[3467]	9.28[t][53]	2.23[s]	6.22[t](5.7)		
[Pd(Me)]Cl (**4cy**)	37.6[s]	8.69[s]	2.23[s]	5.51[b]	0.45[d]{2.6}	
[Pd(Me)]Br (**5cy**)	36.5[b]	9.04[b]	2.34[b]	6.32[b]	0.53[b]	
[Pd(Me)]I (**6cy**)	35.9[s]	8.87[s]	2.23[b]	5.69[b]	0.36[d]{3.3}	
[Pd(Me)]OTf (**7cy**)	42.6[s]	8.59[s]	2.31[b]	5.01[b]	0.63[s]	
[Pd(C(O)Me)]Cl (**12cy**)	19.9[s]	8.71[s]	2.08[s]	5.37[t](6.5)		2.35[s]
[Pd(C(O)Me)]Br (**13cy**)	18.3[s]	8.82[s]	2.12[s]	5.42[b]		2.31[s]
[Pd(C(O)Me)]I (**14cy**)	17.2[s]	9.05[s]	2.16[s]	5.56[b]		2.28[s]
[Pd(C(O)Me)]OTf (**15cy**)	18.4[s]	10.7[s]	2.17[s]	4.96[b]		2.34[s]
	$C^{10}H$	C^1H_3	C^4H	$C^{12}H^w$	$C^{13}H^x$	$C^{14}H^y$	$C^{15}H^z$	Pd–Me	Pd–C(O)Me
NN'S (**d**)	8.25[s]	1.97[s]	3.89[q]	7.71[t]	7.30[t]	7.91[d]	8.59[q]		
[PdCl]Cl (**1dy**)	9.51[s]	2.63[s]	5.40[b]	8.19[t]	7.73[t]	8.48[d]	9.03[d]		
[PdBr]Br (**2dy**)	9.83[s]	2.67[b]	5.59[b]	8.29[t]	7.75[t]	8.59[d]	9.35[d]		
[PtI]I (**3dz**)	10.1[t][95]	2.45[b]	5.87[b]	7.86[t]	7.72[t]	8.25[d]	8.29[d]		
[Pd(Me)]Cl (**4dy**)	8.92[s]	2.43[b]	5.42[b]	8.06[t]	7.70[t]	8.10[d]	8.42[d]	0.57[s]	
[Pd(Me)]Br (**5dy**)	9.57[s]	2.73[b]	5.60[b]	8.19[t]	7.70[t]	8.39[b]	9.34[b]	0.74[s]	
[Pd(Me)]OTf (**7dy**)	8.82[s]	2.56[s]	4.95[b]	8.03[d]	7.73[t]	8.17[t]	8.55[d]	0.76[s]	
[Pd(C(O)Me)]Cl (**12dy**)	8.73[s]	2.29[s]	5.03[b]	7.92[b]	7.62[t]	8.68[t]	8.45[b]		2.63[s]
[Pd(C(O)Me)]OTf (**15dy**)	8.70[s]	2.52[s]	4.84[b]	7.69[t]	7.53[b]	8.01[d]	8.20[d]		2.63[s]

J_{H-H} between (), J_{P-H} between {} and J_{Pt-H} and J_{Pt-P} between []. [b] broad, [s] singlet, [d] doublet, [m] multiplet, [q] quintet. [w] triplet: free ligand: $^3J_{H-H}=6.1$ Hz; complexes: 6.9 Hz $< {}^3J_{H-H} < 7.7$ Hz. [x] triplet: free ligand: $^3J_{H-H}=4.9$ Hz; complexes: 5.8 Hz $< {}^3J_{H-H} < 6.9$ Hz. [y] doublet: free ligand: $^3J_{H-H}=7.8$ Hz; complexes: 6.8 Hz $< {}^3J_{H-H} < 8.0$ Hz. [z] doublet: free ligand: $^3J_{H-H}=4.8$ Hz; complexes: 4.9 Hz $< {}^3J_{H-H} < 5.9$ Hz. At 243 K the $^{31}P\{^1H\}$ NMR ($CDCl_3$) resonances of **4az** are observed at 18.6[3967] (81%) and 15.9[4395] (19%); the ^1H shows: 9.44, 8.58 ($C^{10}H$); 2.40, 2.27 (C^1H_3); 0.14[63], 0.42[54] (Pt–Me). **4cy**: $^{31}P\{^1H\}$ NMR (213 K, $CDCl_3$): 33.2 (12%), 34.2 (13%), 42.1 (56%), 43.5 (19%). **7cy**: $^{31}P\{^1H\}$ NMR (223 K, $CDCl_3$): 41.3 (73%), 42.1 (17%). [x]

respectively (Table 4), which is also supported by the downfield shifts of C(1) ($0.4 < \Delta\delta < 6.8$ ppm), C(10) ($3.2 < \Delta\delta < 10.1$ ppm) and C(15) ($-2.0 < \Delta\delta < 2.8$ ppm) in the $^{13}C\{^1H\}$ NMR spectrum of **2dy**, **4dy** and **5dy** (Section 2), when compared to those values found for the free ligand.

4. Fluxional processes

When considering the molecular structure of **3cz** (Fig. 2) as a reference point we may expect for, e.g. complexes [M(Me)(PNS)]X (M = Pd(II), Pt(II); X = Cl, O_3SCF_3), two different forms when the ligand is terdentate bonded as the six-membered NS containing ring may adopt a boat or a chair conformation. However, at 293 K only one isomer occurs for **4az** which is the major isomer at 243 K as one indeed finds two $^{31}P\{^1H\}$ signals at 18.6 ppm ($J_{Pt-P}=3967$ Hz; 81%) and at 15.9 ppm ($J_{Pt-P}=4395$ Hz; 19%) for the Pt complex [Pt(Me)(PNS-1)]Cl (**4az**) at 243 K, while the Pt bonded methyl group also occurs as two ^1H NMR signals with the same intensity ratio at 0.14 ppm ($^2J_{Pt-H}=63$ Hz; 82%) and at 0.42 ppm ($^2J_{Pt-H}=54$ Hz, $^3J_{P-H}=2.7$; 18%). Two signals were further observed for $C(10)H$ (9.44 and 8.58 ppm) and for $C(1)H_3$ (2.40 and 2.27 ppm). At 293 K the $^{31}P\{^1H\}$ and ^1H signals of Pt–Me, C(10)H and $C(1)H_3$ are in the intermediate exchange. The two diastereoisomers

may have a chair or a boat form in analogy to complexes [PdCl(Me)(NSS')], which contain an η^2-NS bonded NSS' ligand [4].

It is also of interest to compare the chloride complex [Pd(Me)(PNS-3)]Cl (**4cy**) with the analogous triflate complex [Pd(Me)(PNS-3)](O_3SCF_3) (**7cy**). At 223 K, $^{31}P\{^1H\}$ NMR of the latter complex shows two signals at 41.3 (73%) and 42.1 (17%) ppm, which very likely have to be assigned to the two diastereomers described for the platinum complex **4az**. However, in the case of **4cy** in $CDCl_3$ at 213 K four signals are observed at 33.2 (12%), 34.2 (13%), 42.1 (56%) and 43.5 (19%) ppm (Table 4). Since the two latter $^{31}P\{^1H\}$ signals are very close to the chemical shift of the $^{31}P\{^1H\}$ signal of the triflate complex (**7cy**; Table 4) at 293 K, these signals have to be assigned to the two diastereomeric forms of [Pd(Me)(η^3-PNS)]Cl, which interconvert at higher temperatures via an inversion at the sulfur center, thereby causing an interconversion between the boat and the chair forms. It now remains to determine the conformations of the two species with the two higher field signals at 33.2 and 34.2 ppm. Since these values are very close to those found for [PdCl(Me)(η^2-PN)] complexes [20], we tentatively assign these signals to two neutral species with an η^2-PN bonded PNS-3 ligand, which differ with respect to the position of the SR group which may be positioned above the coordination plane or pointing away from the plane (at low temperature), due to hindered rotation around the C(4)–N(1) axis at low temperature by the coordinated Cl atom, as demonstrated by CPK models. Assuming that these assignments are correct we may conclude that the SR group has a rather strong affinity for the palladium atom, as it has a similar affinity for Pd(II) as the chloride anion. The ^1H NMR spectrum of **4cy** was unfortunately not sufficiently informative, as at 213 K no splitting was observed for the $C(1)H_3$ and Pd–Me resonances. However, it was possible to distinguish two broad imine-proton ^1H NMR signals at 8.57 (26%) and 8.90 (74%) ppm which confirms the presence of two different complexes, which are involved in fluxional behavior. This ratio is in any case in accord with the ratios of the $^{31}P\{^1H\}$ signals (i.e. 25 (12+13)% and 75 (56+19)%). At 293 K only one $^{31}P\{^1H\}$ signal is observed for **4cy** at 37.6 ppm. As the weighted mean of the four $^{31}P\{^1H\}$ signals at 213 K lies at 40.3 ppm it is clear that the equilibrium shifts at higher temperatures to the ionic form with the PNS-3 ligand terdentate bonded, as would be expected on entropy grounds and which is also confirmed by the increase of conductivity (Section 2) of 267 Ω^{-1} cm^2 mol^{-1}, measured on **4cy** (vide supra) on going from 223 to 293 K, which is sufficiently close in its properties to $CDCl_3$ in which the NMR spectra were measured.

4.1. [Pd{η^3-allyl}(L)]X (X = Cl, OTf) (8cy–11cy)

Since we are interested in the structural and dynamic features of palladium-allyl complexes with the chiral PNS ligand as compared to the PN [20] and NS [5] complexes, we

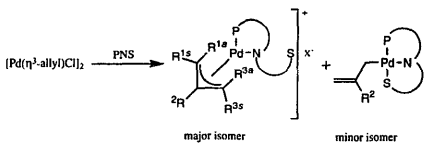

X= Cl X= Otf
8cy, **10cy**, R^2= Me, R^{1s}= R^{1a}= R^{3s}= R^{3a}= H
9cy, **11cy**, R^2= Me, R^{1s}= R^{1a}= Me, R^{3s}= R^{3a}= H

Scheme 3. Numbering of the allyl complexes.

prepared the [Pd{η^3-allyl}(L)]X complexes. However, as insertion of 1,2-propadiene (allene) or 3-methyl-1,2-butadiene (DMA) into the Pd–Me bond of **4cy** failed, these complexes were therefore prepared via an alternative route (Scheme 3). Complexes of the type [Pd{η^3-allyl}(L)][Cl] (**8cy** and **9cy**) were obtained by reacting PNS-3 with [PdX(η^3-allyl)]$_2$, while complexes with X = OTf (**10cy** and **11cy**) were prepared by reaction of **8cy** and **9cy** with AgOTf.

The assignment of both the $^{31}P\{^1H\}$ and ^1H signals was carried out by analogy with the [Pd(η^3-allyl)(PN)]X complexes [20]. Before discussing the allylic palladium complexes we want to draw attention to the general aspects of the spectra obtained. In the first place the number of isomers and isomer concentrations obtained from the $^{31}P\{^1H\}$ NMR spectrum are not always similar to the number and isomer concentrations observed in the ^1H NMR spectra, which is probably due to the inaccuracy of the concentration determination by $^{31}P\{^1H\}$ NMR and the difference in time scales. Therefore the most accurate concentration measurements are based on the imine C(10)H resonance, since these signals are not obscured by other resonances, whereas the allylic resonances, especially the low intensity ones, were frequently obscured by ligand signals.

When discussing these allyl complexes we wish in the first place to draw attention to complex **8cy** which provides rather illuminating results and which therefore may be used as a useful starting point. Firstly, at 293 K two $^{31}P\{^1H\}$ NMR signals have been observed at 25.9 (82%) and 32.3 (18%) ppm (Table 5). This indicates the presence of at least two isomers at 293 K, while at 220 K again two signals occur at 26.0 (79%) and at 33.7 (21%) ppm, which therefore show little temperature dependence of the concentration and of the chemical shifts. The ^1H (Table 6) and $^{13}C\{^1H\}$ NMR spectra at 293 K (Section 2) show downfield shifts of $\Delta\delta(^1H)$ of 0.48 ppm and $\Delta\delta(^{13}C)$ of 2.4 ppm for C(10)H of the major isomer in combination with ^1H and $^{13}C\{^1H\}$ chemical shifts of 1.98 and 14.5 ppm for $C(1)H_3$, which are very close to those of a non-coordinating thioether S atom. These results show that in the case of the major isomer both the phosphorus and the imine-N atom are coordinated, while the methionine thioether arm is dissociated. The allyl group signals occur at 3.86 ppm for the *syn*-protons and at 2.89 ppm for the *anti*-protons, indicating fluxional behavior, with the allyl group η^3-bonded. In the major isomer, therefore, the PNS-3 ligand

Table 5
^{31}P NMR data of **8cy**, **9cy**, **10cy** and **11cy**, recorded in $CDCl_3$

T (K)	Bonding mode of the allyl unit	 (8cy)	 (9cy)	 (10cy)	 (11cy)
293	η^3	25.9 (82%)	25.0 (75%)	26.9 (75%)	26.7 (49%)
	η^1	32.3 (18%)	32.3 (25%)	33.4 (25%)	33.0 (51%)
220	η^3		19.8 (13%)		
			20.9 (13%)		
		26.0 (79%)	24.9 (19%)	26.0 (24%)	24.0 (24%)
			25.7 (9%)	26.2 (49%)	25.2 (11%)
	η^1	33.7 (21%)	33.6 (30%)	33.1 (13%)	32.4 (34%)
			34.1 (16%)	33.9 (14%)	32.7 (31%)

is η^2-PN bonded, while the allyl ligand is η^3-bonded. The ^1H NMR of the minor isomer could not be measured due to the low intensities of the signals. However, the $^{13}C\{^1H\}$ NMR spectrum is more informative and shows allyl ^{13}C signals at 20.8 (C(2)'*Me*), 33.4 (C(1)'), 105.5 (C(3)'), 120.0 (C(2)'), which are typical for an η^1-bonded allyl group, while the signal at 15.1 ppm (C(1)) clearly shows that the sulfur atom of the PNS-3 ligand is now coordinated to the metal.

When considering the fluxional processes it is at this stage useful to note that in the case of major isomer [Pd(η^3-2Me-C_3H_4)(η^2-PNS-3)]Cl (**8cy**) we should expect two diastereomeric forms which differ in the relative position of the η^3-allyl group, which may be up or down with respect to the η^2-PNS-3 bonded ligand, analogous to [Pd(η^3-allyl)(η^2-PN)]Cl [20]. However, at 220 K the $^{31}P\{^1H\}$ signal at 25.9 ppm, which has shifted little from the value at 293 K (Table 5), has not split, indicating the presence of only one diastereomer. This appears to be corroborated by the ^1H NMR spectrum at 220 K, as the two allylic resonances at 293 K have split into four signals, instead of eight if two diastereomers would be present. There is one doublet at 3.72 ppm ($^3J_{P-H}$ = 9.0) for the *anti*-proton *cis* to P, and one doublet at 3.46 ppm ($^3J_{P-H}$ = 9.9 Hz) for the *anti*-proton *trans* to P and a further two signals at 2.67 and 2.90 ppm for the two *syn*-protons. On these last two signals the phosphorus coupling could not be observed owing to some line broadening and overlap with other signals. The two P-coupling constant values on the two *anti*-proton signals are close to each other, but each in the expected range for *anti*-protons *cis* and *trans* to phosphorus [24]. The fluxional process responsible for the coalescence of the four signals to two might involve Berry pseudo-rotational movements occurring in five-coordinate intermediates, while the allyl group remains η^3-bonded to the metal [25]. Such five-coordinate intermediates may be easily visualized, as the anions very likely form short lived ion pairs with the cationic palladium species. An alternative more likely mechanism might involve an intermediate with only the P of the PNS-3 ligand bonded to Pd, analogous to the mechanism proposed by Pregosin and co-workers [26] and Bäckvall and co-workers [27] This intermediate might be stabilized by Cl^- coordination. We should note that the four ^1H signals have coalesced to two, but not at the weighted average, while the $^{31}P\{^1H\}$ signal has changed little in chemical shift on going from 220 to 293 K. This might be due to slightly different configurations of the PNS-3 ligand. The formation of a small amount of the second diastereomer may also be responsible, although less likely in view of the small chemical shift change of the $^{31}P\{^1H\}$ signal with temperature. However, we certainly do not exclude this possibility.

The minor η^1-allyl bonded isomer of **8cy** with the $^{31}P\{^1H\}$ signal at 33.7 ppm at 220 K (Table 5) showed a downfield shift of both the imine C(10)H proton and the $C(1)H_3$ group in ^1H NMR (Table 6) when compared to the values found for the free ligand (Table 4), which shows that the PNS ligand is terdentate bonded. The allylic resonances could unfortunately not be observed, while owing to low signal intensities ^{13}C NMR could not be measured.

In the case of complex **9cy**, which contains an asymmetrically substituted allyl group, the ^{31}P NMR spectrum at 293 K consists of two signals at 25.0 (75%) and 32.3 (25%) ppm (Table 5), which may be assigned to η^3- and η^1-allyl bonded species. This is in accord with the ^1H NMR spectrum which contains a major imine proton signal at 8.84 ppm (69%) together with a $C(1)H_3$ signal at 1.98 ppm due to a dangling methionine thioether arm. The minor imine proton signal at 8.62 ppm (31%) belongs to the η^1-allyl bonded form, as the $C(1)H_3$ signal of the terdentate bonded ligand occurs at 2.12 ppm. The *syn*- and *anti*-protons of the allylic CH_2 moiety of the major isomer have coalesced at 3.82 ppm indicating an η^3–η^1–η^3 fluxional movement [28], while for the minor isomer the Pd–CH_2 protons of the η^1-allyl group absorb as one signal (Table 6: 2.78 ppm), as expected [29]. At 220 K the $^{31}P\{^1H\}$ NMR spectrum consists of six signals, of which the ones at 19.8 (13%), 20.9 (13%), 24.9 (19%) and 25.7 (9%) ppm are clearly due to η^3-allyl bonded species with an η^2-PN bonded PNS-3 ligand. The first two probably belong to the up and down forms of the isomer with the CMe_2 group *trans* to P and the last two signals to the up and down forms of the isomer with the CMe_2 group *cis* to P [20]. The $^{31}P\{^1H\}$ shifts at 33.6 (30%) and 34.1 (16%) ppm have to be ascribed to the two possible η^1-allyl bonded species, which

Table 6
^{1}H NMR data of **8cy**, **9cy**, **10cy** and **11cy**, recorded in $CDCl_3$

	T (K)	al.	H^{10}	Ratio	C^1H_3	C^2H_3	R^{1a}	R^{3a}	R^{1s}	R^{3s}
8cy	293	η^3	8.92[b]	80%	1.98[s]	1.91[b]	2.89[b](H)	2.89[b](H)	3.86[b](H)	3.86[b](H)
		η^1	8.62[b]	20%	2.15[s]		–	–	–	–
	220	η^3	9.01[b]	76%	2.02[b]	1.94[b]	3.72[d][9.0](H)	3.46[d][9.9](H)	2.90[b](H)	2.67[b](H)
		η^1	8.77[b]	24%	2.13[s]	–	–	–	–	–
9cy	293	η^3	8.84[b]	69%	1.98[s]	1.78	1.18[b](Me)	3.82[b](H)	1.76[b](Me)	3.82[b](H)
		η^1	8.62[b]	31%	2.12[s]	1.71[s]	1.22[s](Me)	2.78[b](H)	1.82[s](Me)	2.78[b](H)
	220	η^3	9.31[b]	38%	1.96[s]	1.83[b]	1.40[d][2.5](Me)	2.80[b](H)	1.91[b](Me)	3.85[b](H)
		η^1	8.76[b]	29%	2.09[b]	1.51[s]	–	2.55[b]	–	2.55[b]
			8.46[s]	19%	–	–	–	–	–	–
			8.31[b]	14%	–	–	–	–	–	–
10cy	293	η^3	8.92[b]	81%	2.04[s]	1.78[s]	2.74[b](H)	2.74[b](H)	3.78[b](H)	3.78[b](H)
		η^1	8.55[s]	19%	2.38[s]	–	–	–	–	–
	223	η^3	8.53[s]	28%	2.03[b]	–	3.58[b](H)	–	–	–
		η^3	8.85[b]	39%	2.03[b]	–	3.68[d][8.9](H)	3.22[b](H)	–	–
		η^1	9.08[b]	15%	–	–	–	–	–	–
		η^1	9.32[b]	18%	–	–	–	–	–	–
11cy	293	η^3	8.47[b]	62%	1.98[s]	1.84[s]	1.15[s](Me)	2.77[b](H)	2.01[s](Me)	3.62[b](H)
		η^1	8.55[b]	38%	2.16[s]	1.77[b]	1.09[s](Me)	–	–	–
	220	η^3	8.51[b]	29%	1.85[b]	1.58[s]	–	–	1.95[b]	–
		η^1	8.48[b]	71%	2.22[b]	1.63[s]	0.98[b](Me)	2.93[b](H)	2.03[b](Me)	2.93[b](H)

al. = bonding mode of the allyl unit, [b] broad, [s] singlet, [d] doublet, – = obscured resonance, $^3J_{P-H}$ is between [ ].

probably differ with respect to the position of the S–Me group, which might occur with changes of the NS containing six-membered ring, i.e. either a boat or a chair conformation in analogy to complex **4cy** (vide supra).

The ^1H NMR spectrum of **9cy** at 220 K is unfortunately incomplete owing to the large number of isomers which resulted in low intensities and overlap. We managed to observe four of the expected six imine proton signals (Table 6), but could only assign two at 9.31 ppm with the $C(1)H_3$ at 1.96 ppm as an η^3-allyl species and at 8.76 ppm with $C(1)H_3$ at 2.09 ppm as an η^1-allyl complex.

The $^{31}P\{^1H\}$ NMR spectrum at 293 K of the triflate complex **10cy** shows two signals at 26.6 (75%) and 33.4 (25%) ppm belonging to η^3-allyl and η^1-allyl bonded species, respectively, in analogy to **8cy** (Table 5), which is confirmed by the ^1H NMR spectrum at 293 K (Table 6) which shows an imine proton signal at 8.92 ppm (81%) with a $C(1)H_3$ signal at 2.04 ppm and a C(10)H signal at 8.55 ppm (19%) with a $C(1)H_3$ signal at 2.38 ppm. The chemical shifts at 293 K of the allylic signals, which could only be measured for the major η^3-allyl bonded isomer, shows in analogy to **8cy** a coalescence of the *anti*-protons at 2.74 ppm and of the *syn*-protons at 3.78 ppm. As the triflate anion is a weakly coordinating anion and as therefore five-coordinate intermediates are unlikely, we prefer to rationalize this η^3–η^3 fluxional process by the mechanism proposed by Pregosin [26] and Bäckvall [27] (vide supra). At 220 K four $^{31}P\{^1H\}$ signals have been observed at 26.0 and 26.2 ppm (total 73%) and 33.1 and 33.9 ppm (total 27%) (Table 5). These data, in combination with the ^1H NMR signals (Table 6) for C(10)H at 8.53 and 8.85 ppm (total 67%) with $C(1)H_3$ signals both at 2.03 ppm, and with the C(10)H signals at 9.08 and 9.32 ppm (total 33%), for which the $C(1)H_3$ signals were not observed, show that at 220 K, as expected, two η^3-allyl bonded isomers exist. One of the explanations for the existence of two η^3-allyl bonded isomers lies in the fact that the Me substituent on the $C^{2\prime}$ carbon may point up and down with respect to the chiral ligand backbone of the η^2-PN bonded PNS ligand [30]. There are also two η^1-allyl bonded species with the NS containing metallacycle in a chair or boat form.

Finally, in the case of **11cy** both $^{31}P\{^1H\}$ NMR and ^1H NMR spectra at 293 K (Tables 4 and 5) show similar species as for the other allylic compounds. However, in contrast to **9cy** one observes at 220 K in the $^{31}P\{^1H\}$ NMR spectrum (Table 5) in addition to the two expected signals for η^1-allyl species at 32.4 and 32.7 ppm (total 65%), only two, instead of four, signals at 24.0 and 25.2 ppm (total 35%). Since these signals are comparable to two of the four signals of η^3-allyl species of **9cy** (Table 5), we have to assign these signals to a complex with the CMe_2 moiety **cis** to the P atom, which exists in two isomeric forms, with the central allylic substituent either up or down with respect to the ligand backbone (vide supra). It is rather remarkable that in the ^1H NMR spectrum at 220 K we observe only one imine proton signal at 8.51 ppm (29%) of the η^3-allyl bonded species and one signal at 8.48 ppm (71%) belonging to the η^1-allyl bonded isomer, while two would have been expected for each isomer. The allylic signals of the major species, which are now the η^1-allyl bonded ones, show also the presence of four signals instead of eight with the Pd–CH_2 moiety appearing at 2.93 ppm. These results indicate that even at low temperature the two forms of each isomer, which could be distinguished by $^{31}P\{^1H\}$ NMR (Table 5), are still fluxional on the ^1H NMR time scale.

Finally, it should be noted that based on ^1H NMR and even on the, admittedly less precise, $^{31}P\{^1H\}$ NMR concentration measurements, the amount of the η^3-allyl bonded species increases somewhat with increasing temperature for **8cy** and **10cy**, while a fairly large increase is observed for **9cy** and **11cy** which both contain asymmetrically substituted allyl groups (Tables 4 and 5). This is understandable as this type of allyl group is more prone to become η^1-bonded on the non-substituted end. We have no ready explanation for this shift in equilibrium in the case of **8cy** and **10cy**, but wish only to remark that, as clearly only small energy differences are involved, further discussion is not warranted. It is, however, interesting to note, when taking into account the strong tendency of the allyl group to be η^3-allyl bonded, that in these complexes the existence of η^1-allyl bonded species indicates that the methionine thioether function has a strong affinity for the palladium atom, as has also been noted before (vide supra). Finally, it is interesting that, while there are fast exchange processes occurring within the set of η^2-PNS bonded isomers and within the set of η^3-PNS bonded isomers, there is a relatively slow exchange between both sets indicating a rather large kinetic stability of the methionine thioether S atom, with respect to substitution for all four compounds measured (Tables 4 and 5).

5. Reactions of methylpalladium and -platinum complexes with CO

5.1. [M(C(O)Me)(L)]X (M = Pd, L = PNS, X = Cl, Br, I, OTf; L = NN'S, X = Cl, O_3SCF_3)

To investigate the role of the anions and the ligands on the CO insertion rates we investigated the reactions of complexes **4**, **5**, **6** and **7** with CO under pressure (10 bar) at 293 K which afforded the corresponding acyl complexes **12**, **13**, **14** and **15**, respectively (Scheme 4). The acyl complexes appeared to be rather instable both under CO and N_2, as colloidal palladium or platinum was slowly formed. Upon release of CO pressure decarbonylation occurred at a rate which is similar to the inverse of the half-lives of the carbonylation rates, which made it impossible to carry out $^{13}C\{^1H\}$ and temperature dependent ^1H measurements. Also, since the insertions were performed with a non-spinning 10 mm HP NMR tube (Section 2), no low temperature ^1H NMR spectra could be measured owing to line broadening caused by a low homogeneity of the solution.

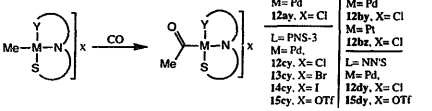

Scheme 4. Numbering of the acyl complexes.

The configuration of the PNS acylpalladium complexes appears to be similar to that of the methyl complexes as the upfield shifts of the ^{1}H imine signals of ligands **a** and **b** relative to the ligand values (Table 4) and the downfield ^{1}H imine shift of ligand **c** clearly show coordination of the imine-N atom, while the downfield shifts of $C(1)H_3$ for all PNS complexes indicate sulfur coordination. Terdentate coordination of the PNS-2 ligand in the case of the acylplatinum complex (**12bz**) is also clear from the $^{31}P\{^1H\}$ and ^{1}H NMR data presented in Table 4.

Also the NN'S ligand is terdentate bonded as the ^{1}H NMR signals of $C(1)H_3$ and of C(10)H shift downfield and C(15)H upfield for complexes **12dy** and **15dy** relative to the free ligand. Since the reaction rates are sufficiently small we have attempted to observe intermediate species. However, these could not be observed; the $^{31}P\{^1H\}$ signal of the PNS methylpalladium complexes slowly disappeared with concomitant formation of the product signal, which is accompanied by the disappearance of the Pd–Me ^{1}H NMR signal and formation of the Pd–C(O)Me signal.

In Fig. 3 it is shown that the insertion reaction is first order with respect to the palladium complex, as has also been observed for [PdX(Me)(η^2-PN)] complexes [20]. From Fig. 3 and from the reactivities expressed by the half-lives of the methyl complexes at 293 K (247 ± 20 min, **4dy**; 200 ± 18 min, **4cy**; 153 ± 22 min, **5cy**; 126 ± 16 min, **6cy**; 135 ± 12 min, **7cy**; 93 ± 16 min, **4by**; 78 ± 19 min, **4ay**), it is clear that the insertion rate increases on going from chloride to iodide, while the highest rate is found for the weakly coordinating

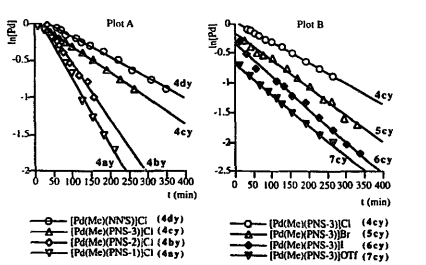

Fig. 3. CO insertion rates obtained at 293 K in $CDCl_3$. Plot A shows the logarithmic decrease of the starting complexes vs. time (min) when 10 bar CO is applied for **4dy**, **4cy**, **4by** and **4ay**. Plot B shows the logarithmic decrease of the starting complexes vs. time (min) when 10 bar CO is applied for **4cy**, **5cy**, **6cy** and **7cy**. The insertion rates (k_{obs}) were calculated using $\ln\{[(C(t)]/[(C(0)]\} = -kt$.

triflate anion, similar to the relative rates observed for [PdX(Me)(η^2-PN)] complexes [20].

This trend is at first sight rather strange, since we would expect for complexes [Pd(Me)(η^3-PNS)]X in principle similar rates if the anion is fully dissociated. However, we have found that we must take into account in solution an equilibrium between this ionic η^3-PNS bonded complex and the neutral [PdX(Me)(η^2-PNS)] (X = Cl, Br, I) (vide supra). In addition we must consider the possibility that the anions will form ion-pairs (vide supra) [20], in which the better coordinating anions might hinder attack of CO on the palladium atom. In any case we note that the rates observed for these complexes are approximately five times slower than measured for the [PdX(Me)(η^2-PN)] complexes [20]. Not unexpected is that with increasing bulk of the substituent on the C(4) atom the rates decrease in the order PNS-1 > PNS-2 > PNS-3. Rather surprising is that complexes [Pd(Me)(NN'S)]X react even slower than the analogous PNS-3 containing complex, while the opposite would have been expected since complexes containing either NN' ligands or NS ligands react rapidly with CO [5].

6. Discussion

As a number of aspects have already been discussed in the results section in sufficient detail we want to focus our attention in particular on the PNS and NN'S ligands in the complexes reported here. Firstly, the PNS and NN'S ligands may be considered to consist of the PN [20] and NS [6] and of the NN' [5] and NS [6] building blocks, respectively, which have been investigated in some detail before. In the case of the complexes [PdX(Me)(η^2-PN)] (PN = 2-(diphenylphosphino)benzylidene-*S*(−)-α-methyl-benzylamine) the P and N atoms are part of a rigid six-membered ring [20]. However, the six-membered chelate NS containing ring in complexes [PdX(Me)(η^2-NS)] (NS = *D*/*L*-methionine-methyl ester, *N*-(thienylidene)-*L*/*D*-methionyl]methyl-ester) [4,6] is very flexible and may adopt both boat and chair conformations. It should therefore not be surprising that the structural and dynamic features of the building blocks are reproduced in the PNS and NN'S ligands.

A remarkable and unexpected feature of the PNS and NN'S ligands is that, when bonded as terdentates to Pd(II) and Pt(II), the S atom is unusually strongly bonded when compared to the NS complexes [PdX(Me)((η^2-NS)] mentioned above.

From the NMR results it is clear that in solution the S-donor atom is able to compete very efficiently with the good coordinating Cl^- anion, as in the major isomer of, for example, **4cy** the PNS-3 ligand is terdentate bonded. Even in the case of the allyl complexes, one of the isomers has the allyl group η^1-bonded with the PNS-3 ligand acting again as a terdentate. This is remarkable in view of the very strong tendency of the allyl group to remain η^3-bonded in the case of palladium compounds [28]. This strong tendency of the

PNS and NN'S ligands to be terdentate bonded might also be the reason that the Pd–Me complexes [Pd(Me)(η^3-PNS)]X and [Pd(Me)(η^3-NN'S)]X react so slowly with CO at room temperature when compared to complexes [PdX(Me)((η^2-NS)] (NS = *D*/*L*-methionine-methyl ester, *N*-(thienylidene)-*L*/*D*-methionyl]methyl ester) which react very fast indeed with CO [4,6]. This was in the case of these complexes tentatively rationalized by a temporary dissociation of the S atom, which is in analogy to complexes [PtX(Me)-(PN)] (PN = 1-dimethylamino-8-diphenylphosphinonaphthalene, 1-dimethylamino-3-diphenylphosphinopropane) for which it was unequivocally shown that the N atom, for both rigid and flexible PN ligands, is dissociated during the insertion process [31]. It appears therefore clear that the *trans*-group which is PPh_2 in the case of PNS and the pyridine moiety in the case of the NN'S ligand is responsible for the apparent strong Pd–S bond. Since both moieties are reasonably good π-acceptors, while the thioether S-donor group is a good π-donor we may rationalize the strong Pd–S bond by a well balanced electronic push–pull effect. Such an electronic push–pull mechanism has also been proposed to explain the strong tendency for the PNN' ligand *N*-(2-diphenylphosphinobenzylidene)-2-(2-pyridyl)ethylamine [29] and for the NN'N'' ligand 2-(2,2'methylidene-*N*-methylimidazolyl)aminoethyl(pyridine) [32] to behave as a terdentate towards Pd(II).

7. Supplementary material

Further details of the structure determinations, including atomic coordinates, bond lengths and angles, and thermal parameters (25 pages) are available from the authors on request.

Acknowledgements

This work was supported by the Netherlands Foundation of Chemical Research (SON) with financial aid from the Netherlands Organisation for Scientific Research (NWO) (A.L.S.) and by the award of a postdoctoral fellowship under the EC Human Capital and Mobility initiative (M.T.L.). Thanks are due to J.-M. Ernsting for support in collecting the NMR data, M.G. Oostenbrink for synthetic support and Professor C.J. Elsevier for his interest and suggestions.

References

[1] (a) P.M. Colman, H.C. Freeman, J.M. Guss, M. Murata, V.A. Norris, J.A.M. Ramshaw and M.P. Venkatappa, *Nature, 272* (1978) 319; (b) J.M. Guss and H.C. Freeman, *J. Mol. Biol., 169* (1983) 521; (c) J.M. Guss, P.R. Harrowell, M. Murata, V.A. Norris and H.C. Freeman, *J. Mol. Biol., 192* (1986) 361.

[2] J.F. Modder, K. Vrieze, A.L. Spek and G. van Koten, *J. Org. Chem., 56* (1991) 5606.

[3] J.F. Modder, G. van Koten, K. Vrieze and A.L. Spek, *Angew. Chem., Int. Ed. Engl., 28* (1989) 1698.

[4] H.A. Ankersmit, P.T. Witte, H. Kooijman, M.T. Lakin, A.L. Spek, K. Goubitz, K. Vrieze and G. van Koten, to be published.

[5] R.E. Rülke, M. Han, C.J. Elsevier, K. Vrieze, P.W.N.M. van Leeuwen, C.F. Roobeek, M.C. Zoutberg, Y.F. Wang and C.H. Stam, *Inorg. Chim. Acta, 169* (1990) 5.

[6] H.A. Ankersmit, N. Veldman, A.L. Spek, K. Eriksen, K. Goubitz, K. Vrieze and G. van Koten, *Inorg. Chim. Acta, 252* (1996) 203.

[7] H.C. Freeman and M.L. Golomb, *J. Chem. Soc., Chem. Commun.,* (1970) 1523.

[8] R.C. Warren, J.F. McConnel and N.C. Stephenson, *Acta Crystallogr., Sect. B, 26* (1970) 1402.

[9] R. Rülke, J.M. Ernsting, A.L. Spek, C.J. Elsevier, P.W.N.M. van Leeuwen and K. Vrieze, *Inorg. Chem., 32* (1993) 5769.

[10] T.B. Rauchfuss and D.A. Wrobleski, *Inorg. Synth., 21* (1982) 175.

[11] (a) W. Schneider, *Liebig's Anal. Chem., 177* (1910) 245; (b) P. Karrer, E. Scheitlin and H. Siegrist, *Helv. Chim. Acta, 159* (1950) 1237.

[12] H. Itoh, D. Hagiwara and T. Kamiya, *Tetrahedron Lett., A23* (1975) 312.

[13] C.J. Elsevier, *J. Mol. Catal., 92* (1994) 285.

[14] J.L. de Boer and A.J.M. Duisenberg, *Acta Crystallogr., Sect. A, 40* (1984) C410.

[15] A.L. Spek, *J. Appl. Crystallogr., 21* (1983) 578.

[16] N. Walker and D. Stuart, *Acta Crystallogr., Sect. A, 39* (1983) 158.

[17] P.T. Beurskens, G. Admiraal, G. Beurskens, W.P. Bosman, S. García-Granda, R.O. Gould, J.M.M. Smits and C. Smykalla, The DIRDIF program system, *Tech. Rep.,* Crystallography Laboratory, University of Nijmegen, Netherlands, 1992.

[18] G.M. Sheldrick, *SHELXL-93,* program for crystal structure refinement, University of Göttingen, Germany, 1992.

[19] A.L. Spek, *Acta Crystallogr., Sect. A, 46* (1990) C34.

[20] H.A. Ankersmit, B.H. Løken, H. Kooijman, A.L. Spek, K. Vrieze and G. van Koten, *Inorg. Chim. Acta, 252* (1996) 141.

[21] J.C. Jeffery, T.B. Rauchfuss and P.A. Tucker, *Inorg. Chem., 19* (1980) 3306.

[22] (a) D.P. Arnold, M.A. Bennet, M.S. Bilton and G.B. Robertson, *J. Chem. Soc., Chem. Commun.,* (1982) 115; (b) A.J. Blake, R.O. Gould, A.J. Lavery and M. Schröder, *Angew. Chem., Int. Ed. Engl., 25* (1986) 274; (c) S. Fallis, G. Anderson and N.P. Rath, *Organometallics, 10* (1991) 3180; (d) F.P. Fanizzi, F.P. Intini, L. Maresca, G. Natile, M. Lanfranchi and A. Tiripicchio, *J. Chem. Soc., Dalton Trans.,* (1991) 1007; (e) H.-K. Yip, L.-K. Cheng, K.-K. Cheung and C.-M. Che, *J. Chem. Soc., Dalton Trans., 19* (1993) 2933; (f) C.A. Ghilardo, S. Midollini, A. Orlandini, G. Scapacci and A. Vacca, *J. Organomet. Chem., 461* (1993) C4; (g) T. Tanase, H. Ukaji, Y. Kudo, M. Ohno, K. Kobayashi and Y. Yamamoto, *Organometallics, 13* (1994) 1374; (h) R.H. Herber, M. Croft, M.J. Coyer, B. Bilash and A. Sakiner, *Inorg. Chem., 33* (1994) 2422.

[23] R. Rülke, J.M. Ernsting, A.L. Spek, C.J. Elsevier, P.W.N.M. van Leeuwen and K. Vrieze, *Inorg. Chem., 32* (1993) 5769.

[24] P.S. Pregosin and R.W. Kunz, in P. Diehl, E. Fluck and R. Kosfeld (eds.), *NMR Basic Principles and Progress,* Springer, Heidelberg, 1979, p. 28.

[25] (a) K. Vrieze, P. Cossee and A.P. Praat, *Recl. Trav. Chim. Pays-Bas, 86* (1967) 769; (b) S. Hansson, P-O. Norrby, M.P.T. Sjörgen, B. Åkermark, M.E. Cucciolito, F. Giordano and A. Vitagliano, *Organometallics, 12* (1993) 4940.

[26] A. Albinati, R.W. Kunz, C.J. Ammann and P.S. Pregosin, *Organometallics, 10* (1991) 1800.

[27] A. Gogoll, J. Örnebro, H. Grennberg and J.E. Bäckvall, *J. Am. Chem. Soc., 116* (1994) 3631.

[28] (a) K. Vrieze, P. Cossee and A.P. Praat, *Recl. Trav. Chim. Pays-Bas, 86* (1967) 769; (b) K. Vrieze, P. Cossee, A.P. Praat and C.W. Hilbers, *J. Organomet. Chem., 11* (1968) 353; (c) S. Hansson, P-O. Norrby, M.P.T. Sjörgen, B. Åkermark, M.E. Cucciolito, F. Giordano and A. Vitagliano, *Organometallics, 12* (1993) 4940.

[29] R.E. Rülke, V.E. Kaasjager, P. Wehman, C.J. Elsevier, P.W.N.M. van Leeuwen, K. Vrieze, J. Fraanje, K. Goubitz and A.L. Spek, *Organometallics*, submitted for publication.

[30] C. Breutel, P.S. Pregosin, R. Salzman and A. Togni, *J. Am. Chem. Soc., 116* (1994) 4067.

[31] G.P.C.M. Dekker, A. Buijs, C.J. Elsevier, K. Vrieze, P.W.N.M. van Leeuwen, W. Smeets, A.L. Spek, Y.F. Wang and C. Stam, *Organometallics, 11* (1992) 1937.

[32] R.E. Rülke, V.E. Kaasjager, D. Kliphuis, C.J. Elsevier, P.W.N.M. van Leeuwen, K. Vrieze and K. Goubitz, *Organometallics*, in press.